Hindawi Publishing Corporation
Journal of Spectroscopy
Volume 2013, Article ID 951604, 26 pages
http://dx.doi.org/10.1155/2013/951604

Review Article

Spectroscopic Characterization of Poly(*ortho*-Aminophenol) Film Electrodes: A Review Article

Ricardo Tucceri,[1] Pablo Maximiliano Arnal,[2] and Alberto Néstor Scian[2]

[1] *Instituto de Investigaciones Fisicoquímicas Teóricas y Aplicadas (INIFTA), Facultad de Ciencias Exactas, Universidad Nacional de La Plata, Sucursal 4, Casilla de Correo 16, 1900 La Plata, Argentina*
[2] *Centro de Tecnología de Recursos Minerales y Cerámica (CETMIC), CIC-CONICET La Plata, Buenos Aires Casilla de Correo 49, B1897ZCA Manual B. Gonnet, Argentina*

Correspondence should be addressed to Ricardo Tucceri; rtucce@gmail.com

Received 14 June 2012; Revised 25 August 2012; Accepted 8 September 2012

Academic Editor: Feride Severcan

This paper refers to spectroscopic studies carried out to identify the products of *o*-aminophenol electro-oxidation and elucidate the structure of electrochemically synthesized poly(*o*-aminophenol) (POAP) films. Spectroscopic studies of the redox conversion of POAP are also reviewed.

1. Introduction

The oxidation of *ortho*-aminophenol (*o*-AP) on different electrode materials (gold, platinum, carbon, indium tin oxide, etc.) in aqueous medium was shown to form poly(*ortho*-aminophenol, (POAP). Like aniline, *o*-AP can be polymerized electrochemically in acidic, neutral, and alkaline solutions. Table 1 lists the electrode materials, electrosynthesis methods, and electrolyte composition employed by different authors to obtain POAP films [1–13]. The electropolymerization of *o*-AP in acid medium yields an electroactive polymer that exhibits its maximal electroactivity within the potential range $-0.2\,\text{V} < E < 0.5\,\text{V}$ (*versus* SCE) at pH values lower than 3 [14, 15]. The electroactivity of POAP was explained by a redox mechanism that involves an addition/elimination of protons coupled with a reversible electron transfer [15]. The charge-transport process at POAP films was studied by employing different electrochemical techniques [14–23], and it was found that it depends not only on the medium used for the electrosynthesis, but also on the polymer oxidation state, the polymer film thickness, pH, and type of ions of the external solution in contact with the polymer [16]. In general, POAP shows a relatively low conductivity [6, 14–18, 21] as compared with other conjugated polymers [24–33] (Table 2). Particularly, the electro-oxidation of *o*-AP in neutral buffer solutions leads to the formation of a non-conducting and permselective thin film of POAP [34]. The permselectivity of a non-conducting POAP film synthesized at pH values over 3 was found to be suitable to reduce the effect of interferents, such as ascorbic acid, uric acid, and acetaminophen in amperometric determinations of different biologically important substances. Besides, the thickness of a non-conducting POAP film is self-controlled during electropolymerization, and a very thin and uniform film can be obtained. These characteristic properties of POAP synthesized in neutral media (thickness uniformity, compactness, and low permeability) have been usefully employed in the development of different types of biosensors. Table 3 lists detection solutions and response characteristics of the different biosensors based on POAP. As can be seen from Table 3, a thin non-conducting POAP film is able to immobilize biological macromolecules, such as glucose oxidase (GOx). The electrochemical immobilization of the enzyme in POAP is typically carried out by potential cycling or at a constant potential by using a phosphate or acetate buffer solution containing the monomer (*o*-AP) and GOx [34]. Although glucose biosensors are mostly obtained by entrapment of GOx in electropolymerized conducting films of polypyrrole (Ppy) [35, 36] and its derivatives [37] and polyaniline (PANI) [38], non-conducting POAP films are generally found to be

Table 1: Electropolymerization of *o*-aminophenol on different electrode materials and in different electrolyte media.

Electrode materials	Electrolyte medium	Electrosynthesis method	Reference
Pt, Au and glassy carbon	0.1 M $HClO_4$ + 0.4 M $NaClO_4$ + 1×10^{-3} M *o*-AP ($1 < pH < 7$)	Potentiodynamic cycling −0.25 V and 0.70 V (SCE)	[1]
Pt electrode	0.4 mol cm^{-3} of $NaClO_4$ + 10^{-2} mol dm^{-3} of *o*-AP	Potentiodynamic cycling −0.25 V and 0.75 V (SCE)	[2]
Carbon paste electrode	5 mM *o*-AP + 0.5 M $HClO_4$ In the presence and in the absence of sodium dodecyl sulfate	Potentiodynamic cycling −0.1 V and 0.7 V (Ag/AgCl/KCl 3 M)	[3]
Platinum and glassy carbon electrodes	0.2 M $NaClO_4$ + 0.1 M $HClO_4$ + 5×10^{-3} M *o*-AP solution	Potentiodynamic cycling 0.2 V and 1.3 V (RHE)	[4]
Glassy carbon electrodes chemically (nitric acid (67% wt/wt) and sulfuric acid (98% wt/wt) for 10 min) and electrochemically (1.85 V (SCE) for 5 min) pretreated before electropolymerization of *o*-AP	0.1 M H_2SO_4 + 0.05 M *o*-AP	Potentiodynamic method (−0.2 V and 0.7 V versus SCE)	[5]
Basal-plane pyrolytic graphite and In-Sn oxide conducting glass	0.5 M Na_2SO_4 solution (pH 1) + 50 mM *o*-AP	Potentiodynamic cycling (−0.4 and 1.0 V versus sodium chloride saturated calomel electrode)	[6]
Glassy carbon	1 M SO_4H_2 + 0.5 M Na_2SO_4 + 50 mM *o*-AP solution	Potentiodynamic cycling (−0.2 V and 1.0 V versus SCE)	[7]
Glassy carbon and Pt electrodes	0.05 M *o*-AP in a mixture of 1 M H_2SO_4 and 0.5 M Na_2SO_4	Potentiodynamic cycling (−0.2 V to 0.8 V versus SCE)	[8]
Pt and Au electrodes	0.05 M *o*-AP + 0.5 M H_2SO_4 solution	Potentiostatic method (E = 0.7 V; 0.8 V and 0.9 V versus SCE	[9]
Pt and GC electrodes	0.05 M *o*-aminophenol solution in 0.5 M $HClO_4$ + 10 mM sulfonated nickel phtalocyanine	Potentiodynamic cycling (−0.25 and 0.7 V versus SCE)	[10]
GC electrodes	0.10 M $HClO_4$ + 0.10 M *o*-AP	Potentiodynamic (−0.10 V and 1.00 V versus SCE) and potentiostatic (E = 1.0 V for a given time) methods	[11]
Vitreous carbon, platinum, and copper	0.3 M NaOH hydroalcoholic solution (70 vol% H_2O, 30 vol% CH_3OH) + 0.1 M *o*-AP	Potentiodynamic cycling	[12]
Glassy carbon electrode or on a glass plate covered with semiconducting indium thin oxide	1 M phosphate buffer solution (pH 5.55) containing 25 μg/mL of laccase and 10 mM *o*-AP	Potentiodynamic cycling (−0.1 V and 0.9 V versus Ag/AgCl)	[13]

more effective than the conducting ones in both preventing the biosensor from fouling and eliminating the interference from electroactive species. Besides, biosensors based on POAP generally have the advantages of fast response and high sensitivity because of relatively high enzyme loading. Thin non-conducting POAP films can also be combined with different electroactive materials (carbon nanotubes, other polymers such as poly(*o*-phenylenediamine) and polypyrrole, hemoglobin, Prussian blue, etc.) to build different biosensors [39–47].

Despite the 2 previous reviews about charge conduction [16] and practical applications [48] of POAP film electrodes reported in the literature, it is expected that this brief review about spectroscopic studies carried out to characterize the products formed during the electropolymerization of *o*-AP, and the species involved in the redox process of POAP will contribute to a more deeper knowledge of the characteristic properties of this polymer.

Table 2: Conductivity of some typical electroactive polymers.

Polymer	[a]Conductivity (Scm^{-1}) of the oxidized polymer	Reference(s)
Poly(*o*-aminophenol)	10^{-7}–10^{-6}	[6, 14–18, 21]
Polyacetylene	3–1000	[24–26]
Polyaniline	0.01–5	[27–29]
Polypyrrole	0.3–100	[29–31]
Polythiophene	2–150	[29, 32]
Poly(*p*-phenylene)	10–500	[29, 33]

[a]Significantly higher conductivity have been published for the polymers listed but not in the context of their practical applications.

Table 3: Detection solutions and response characteristics of the different biosensors based on poly(*o*-aminophenol).

Biosensor	Detection solution	Electrochemical conditions and response characteristics	Detection limit	Reference
Pt/PB/POAP/GOx	1/15 M phosphate buffer solution (pH 7) containing different glucose concentrations (0–35 mM)	Operating potential, $E = 0.6$ V (versus SCE). Linear dependence of the current on glucose concentration up to 5 mM	0.01 mM	[39]
Pt/POAP/GOx	1/15 M phosphate buffer solution (pH 7) containing different glucose concentrations (0–60 mM)	Operating potential, $E = 0.6$ V (versus SCE). Linear dependence of the current on glucose concentration up to 10 mM	0.02 mM	
GC/BCNT/POAP-GOx	1/15 M phosphate buffer solution (pH 7) containing different glucose concentrations (0–25 mM)	Operating potential, $E = 0.6$ V (versus SCE). Linear dependence of the current on glucose concentration up to 8 mM	3.6 μM	[40]
Au/POAP/CNT/GOx	1/15 M phosphate buffer solution (pH 7) containing different glucose concentrations (0–50 mM)	Operating potential, $E = 0.75$ V (versus SCE). Linear dependence of the current on glucose concentration up to 5 mM	0.01 mM	[41]
Au/POAP/GOx	1/15 M phosphate buffer solution (pH 7) containing different glucose concentrations (0–50 mM)	Operating potential, $E = 0.75$ V (versus SCE). Linear dependence of the current on glucose concentration up to 10 mM	0.02 mM	
PGCE/POAP/GOx	A stirred air-saturated 0.05 M phosphate buffer solution (pH 7), where aliquots of glucose were added.	Operating potential, $E = 0.6$ V (versus SCE). The linear response of the enzyme electrode to glucose was from 1×10^{-6} to 1×10^{-3} M	5×10^{-7} M	[41]
POAP-GOx/PPy-Pt/GCE	Stirred solution containing 25 mL air-saturated 0.1 M PBS, pH 7, where glucose was injected using a microsyringe	Operating potential, $E = 0.60$ V (versus SCE). Linear dependence of the current on glucose concentration from 0.0015 mM to 13 mM.	0.45 μM	
POAP-GOx/Pt/GCE	Stirred solution containing 25 mL air-saturated 0.1 M PBS, pH 7, where glucose was injected using a microsyringe	Operating potential, $E = 0.60$ V (versus SCE). Linear dependence of the current on glucose concentration from 0.0042 mM to 12 mM.	0.90 μM	[42]
POAP-GOx/PPy/GCE	Stirred solution containing 25 mL air-saturated 0.1 M PBS, pH 7, where glucose was injected using a microsyringe	Operating potential, $E = 0.60$ V (versus SCE). Linear dependence of the current on glucose concentration from 0.0055 mM to 12 mM.	0.95 μM	
Hb/POAP/FeCoHCF/Au	Aliquots of a standard solution of H_2O_2 added to an acetate buffer solution (pH 5.29)	Operating potential, $E = -0.25$ V (versus SCE). Linear dependence of the current on the H_2O_2 concentration within the range 1.73×10^{-5} M–4.03×10^{-3} M	1.2×10^{-5} M	[43]
HRP-ferrocene/POAP	Batch mode: hydrogen peroxide in 0.1 M phosphate solution (pH 8)	Rotating Disc Electrode Voltammetry (RDEV). Linear dependence of the current on the H_2O_2 concentration within the range 1×10^{-8} M–1×10^{-5} M. Detection potential: 0.050 V (Ag/Ag/Cl)	8.5×10^{-9} M	[44]
	Flow injection mode (FIA): hydrogen peroxide in 0.1 M phosphate solution (pH 8)	Consecutive injections (50 injections per day for six days). Linear dependence of the current on the H_2O_2 concentration within the range 1×10^{-8} M–2×10^{-6} M. Detection potential: 0.050 V (Ag/Ag/Cl)	8.5×10^{-9} M	

Table 3: Continued.

Biosensor	Detection solution	Electrochemical conditions and response characteristics	Detection limit	Reference
Carbon paste/ HRP-Uricase/POAP	A stirred 0.1 M solution of phosphate buffer (pH 7.5) containing uric acid.	Operating potential, $E = 0.050$ V (versus Ag/AgCl). Linear response up to 1×10^{-4} M of urate	3.14×10^{-6} M	[45]
Carbon paste/ HRP-Uricase/POAP	Flow injection system: carrier stream was 0.1 M phosphate buffer (pH 7.5).	Operating potential, $E = 0.050$ V (versus Ag/AgCl). Linear response up to $1 \times 2 \times 10^{-4}$ M of urate. Flow rate 0.85 mL min^{-1}.	6.8×10^{-6} M	
Carbon paste/GPT-LDH-NAD^+/PPD-POAP	0.1 M phosphate, 0.01 M glutamate solution, pH 9.5, containing lactate	Operating potential, $E = 0.0$ V (versus Ag/AgCl). Linear response to lactate up to 8.5×10^{-5} M.	6×10^{-7} M	[46]
Carbon paste/POAP	0.1 M acetate buffer solution (pH 5) or 0.1 M phosphate buffer (pH 7) solution, where NADH was added in increments of 1×10^{-8} M.	Operating potential, $E = 0.15$ V (versus Ag/AgCl). Linear response of the catalytic oxidation current from 0 M to 1×10^{-7} M (NADH)	1.0×10^{-9} M	[47]

2. Spectroscopic Studies of the *o*-AP Electropolymerization Process in Acid Medium

Barbero et al. [1] reported a study about the oxidation of *o*-AP and closely related compounds employing electrochemical, chemical, and spectroscopic measurements. The electrooxidation of *o*-AP was studied on different electrode materials (Pt, Au, and glassy carbon) and different electrolyte media ($1 < pH < 7$). A typical voltammogram of a Pt electrode contacting a 0.1 M $HClO_4$ + 0.4 M $NaClO_4$ + 1×10^{-3} M *o*-AP aqueous solution (pH 1) is shown in Figure 1.

On the first positive sweep, two peaks are defined: **a**, at 0.60 V (SCE) attributed to the oxidation of *o*-AP to monocation radical (*o*-$AP^{\bullet+}$), and **b**, at 0.85 V, which was assigned to the oxidation of (*o*-$AP^{\bullet+}$) to dication. On the negative sweep, none of these peaks show complementary peaks, indicating chemical follow-up reactions giving products detected as peaks **c**-**c**′ and **d**-**d**′ on the subsequent sweeps. It was observed that the system **c**-**c**′ diminishes after continuous cycling in the same way as in **a**, but the peak system **d**-**d**′ increases and shows the characteristic behaviour of a deposited electroactive substance. This was verified by stirring the solution while cycling, because the system **d**-**d**′ remained unchanged, as expected for an irreversibly adsorbed electroactive substance. Analysis of the products employing IR and UV-Vis spectroscopy showed that the couple **d**-**d**′ (Figure 1) corresponds to a polymer of 3-aminophenoxazone (3-APZ). The electroactive substance formed by oxidation of *o*-AP was denominated poly-*o*-aminophenol (POAP). Barbero et al. [1] also prepared the electroactive polymer by chemical oxidation of *o*-AP, and its properties were compared with those of the electrochemically produced POAP. The chemical synthesis of POAP confirmed that the actual monomer in the formation of the polymer is the cyclic dimer of *o*-AP, 3APZ. In this regard, the IR spectrum of an electrochemically prepared POAP film and that of 3APZ were compared (Figure 2).

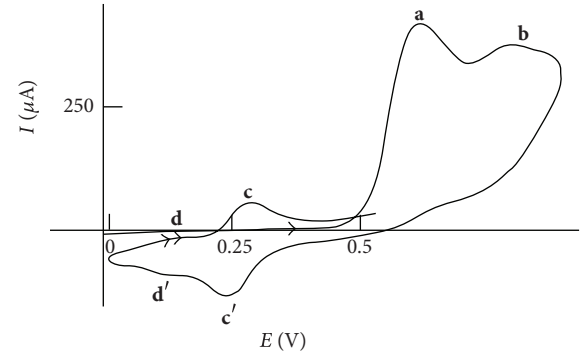

Figure 1: Cyclic voltammogram of a Pt electrode contacting a 0.1 M $HClO_4$ + 0.4 M $NaClO_4$ + 1×10^{-3} M *o*-AP solution, pH 1. Scan rate, $\nu = 0.1$ V s^{-1} and electrode area $A = 0.126$ cm^2 [1].

The broad band centered at 3400 cm^{-1} was assigned to the stretching of the N–H bonds, while the bands at 1350 and 1240 cm^{-1} were ascribed to the –C–N–C– stretching of the secondary amines (Figure 2(a)). Although the stretching of the C=N bond was observed at 1633, 1462, and 1384 cm^{-1}, some of these bands were also assigned to the C–C bond. The characteristic =C–C=O stretching in 3APZ at 1573 cm^{-1} (Figure 2(b)) only appears as a weak absorption in the POAP. This band in POAP was assigned to a terminal group. The C–O (1201 cm^{-1}) and the –C–O–C symmetric stretching vibrations are very well defined in POAP. The peak at 800 cm^{-1} was assigned to the –C–H bending vibration of aromatic *ortho*-substituted aromatic rings. The peak at 1092 cm^{-1} was ascribed to the ClO_4^- band. However, this last peak was associated with an impurity because it disappeared after exhaustive washing of the film. Barbero et al. [1] pointed out the absence of the characteristic strong absorption of carbonyl group (1680 cm^{-1}) and phenol group (2600 cm^{-1}) in the POAP spectrum. The absence of the carbonyl band was considered to be an indication of an insignificant quantity

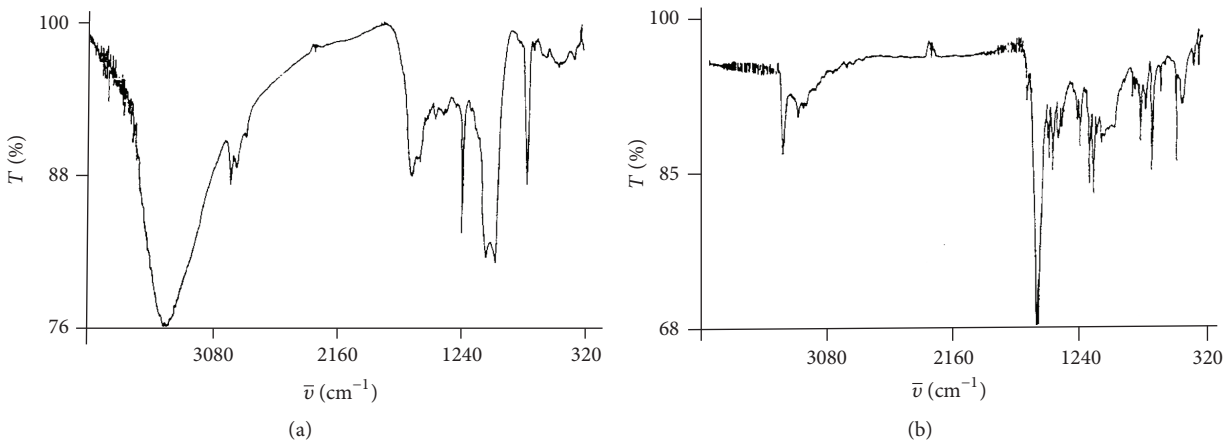

Figure 2: IR spectra of (a) electrochemically prepared POAP and (b) 3-aminophenoxazone [1].

of *o*-quinone in the film. In the same way, the absence of an important hydroxyl group absorption band was attributed to a low proportion of a possible linear chain polymer structure (see below). The POAP structure was also studied by in situ UV-visible spectroscopy in [1]. A broad maximum around 480 nm was observed in the oxidized state of POAP. As the UV-Vis spectrum has the same characteristics as that reported for 3APZ, it was considered as a confirmation that the film is composed of phenoxazine-like units. Then, on the basis of chemical, IR, and UV-visible spectroscopic analyses, the mechanism shown in Figure 3 was proposed for the electrochemical oxidation of *o*-AP.

Barbero et al. [1] propose that a radical cation o-AP$^{+\bullet}$ is formed in a first charge-transfer step, and, then, it may follow the reaction paths shown in Figure 3. The o-AP$^{+\bullet}$ radical may dimerize by either C–C coupling or C–N coupling to give species (I) and (II), respectively. The dimers are oxidized to the corresponding dications. The oxidized dimer II can undergo a cyclization reaction to give species III, which is further oxidized to 3APZ. The product distributions analyzed in [1] allowed the authors to establish that the rate constants for dimer formation follow the order $k_{\mathrm{dI}} < k_{\mathrm{dII}}$ and both rate constants are higher than the cyclization rate (k_c) to give species III. However, the rate of polymerization (k_p) to obtain the immobilized couple on the electrode surface was lower than the cyclization rate (k_c). The possibility that the dication of compound II can polymerize was not disregarded. Then, the formation of a composite of two different films, one of linear chain structure similar to PANI and the other with a phenoxazine-like chain structure, was assumed to be possible. The latter product was considered to be the predominant one in [1]. The POAP redox switching proposed in [1], including oxidized and reduced forms, is shown in Figure 4.

Barbero et al. [1] claim that if extreme care is not taken in the preparation of a POAP film, not only in the concentration but also in the potential ranges, the possibility of side reactions and consequently "side" polymers increases, and the real structures of the films obtained could be quite complex. Then, the best conditions proposed in [1] for obtaining a reproducible POAP film are the repetitive cycling between −0.25 V and 0.70 V (SCE) of an *o*-AP aqueous acid solution (pH 1) and an *o*-AP concentration less than 20 mM.

In order to clarify the structure of POAP, Salavagione et al. [49] studied the electrochemical oxidation of *o*-AP, phenoxazine, and the polymer formed by oxidation of *o*-AP by in situ FTIR spectroscopy. To check whether the observed bands are due to hydrolysis products, FTIR spectra were recorded in both water and deuterated water as solvents.

The spectra of a 1 M $HClO_4$ + 5×10^{-3} M *o*-AP solution, where a polycrystalline platinum electrode immersed in it was polarized at different potential values, are shown in Figure 5. The electrode was immersed in the spectroelectrochemical cell at 0.1 V (RHE), and, then, the potential was stepped up to 0.4 V, and the reference spectrum was collected. The potential was then polarized at higher values to oxidize the *o*-AP, and the sample spectra were acquired at 0.8 V and 1.0 V. In the spectrum at 0.8 V (RHE) (Figure 5(a)) two positive bands at 1510 and 1471 cm^{-1} were observed. These two bands were assigned to the aromatic C=C stretching vibration and ring C=C vibration of *meta*-disubstituted benzenes (see Figures 6 and 3). The positive character of these bands was attributed to consumption of the species related to these features at the sample potential. These two bands at 1.0 V (Figure 5(b)) were observed together with a strong band at 2345 cm^{-1} corresponding to the formation of CO_2 in the solution. No clear bands were observed at lower sample potentials. When the same spectrum was collected in deuterated water (Figure 5(c)), that is, under reduced interference of water absorptions, two negative bands at 1683 and 1645 cm^{-1} were observed. These bands were associated with the C=O and C=N stretching vibrations, respectively.

The spectra of POAP in 1 M $HClO_4$ solution in the absence of *o*-AP, in water and deuterated water, are shown in Figures 7(a) and 7(b), respectively. Again, the reference spectrum was obtained at 0.1 V, so it contains the vibrational information corresponding to the reduced form of the film. The electrode was then polarized at 0.7 V (RHE), and the sample spectrum was collected. Similar bands were observed in both spectra. Figure 7(a) displays two clear positive

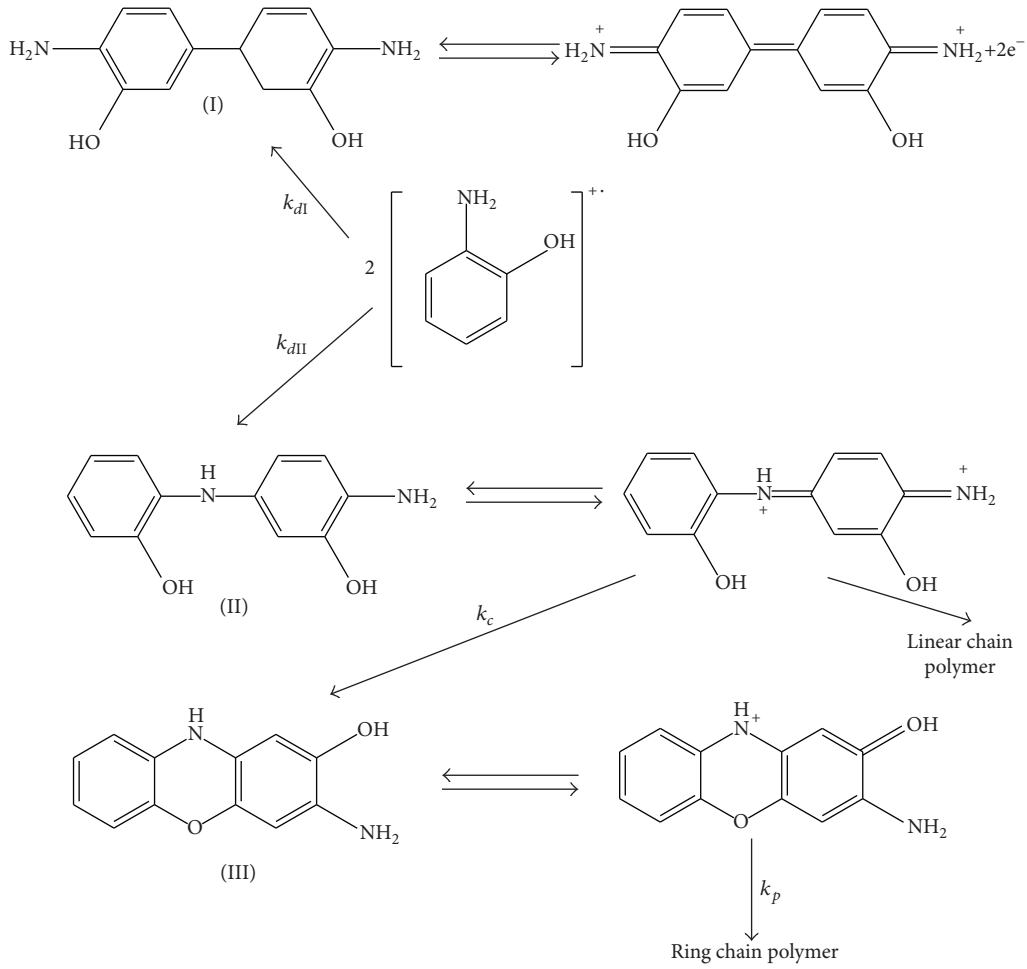

Figure 3: Mechanism of electrochemical oxidation of *o*-AP [1].

Figure 4: Reaction scheme of POAP redox switching including oxidized and reduced forms [1].

bands at 1513 and 1278 cm^{-1} and a broad negative band at 1580 cm^{-1}. The band at 1513 cm^{-1} is also present in the spectra in D_2O (Figure 7(b)), but, in this case, it was observed at 1517 cm^{-1} and was assigned to the C=C stretching of the aromatic ring. This band was not observed after polymer oxidation. The broad negative band at 1580 cm^{-1} was also present in deuterated water, but, in this case, the band has contributions from several bands at 1564, 1606, and 1648 cm^{-1} and was assigned to a quinoid ring or C=N stretching vibration in the phenoxazine units produced upon complete polymer oxidation (Figure 4). The 1648 cm^{-1} band was attributed to C=N stretching where conjugation with phenyl group shifts its frequency to higher values, and it was more clearly observed in deuterated water due to the reduced interference of water absorptions. Another negative band was observed at 1330 cm^{-1} in both spectra, which was also clearly seen at low potentials. This band was assigned to C=N stretching of quinoid rings containing C=N and C–N groups. In order to check these assignments, the spectra for phenoxazine in the same range of potentials were also obtained in [49]. Figure 7(c) shows the spectrum obtained from a 1 M $HClO_4$ + 5×10^{-4} phenoxazine solution in deuterated water, where the polycrystalline platinum electrode immersed in it was polarized at different potential values. A series of reference and sample spectra were collected at 0.2 and 0.7 V and then coadded. The spectrum obtained showed a sharp and negative band at 1508 cm^{-1} corresponding to the disappearance of the aromatic ring at the sample potential.

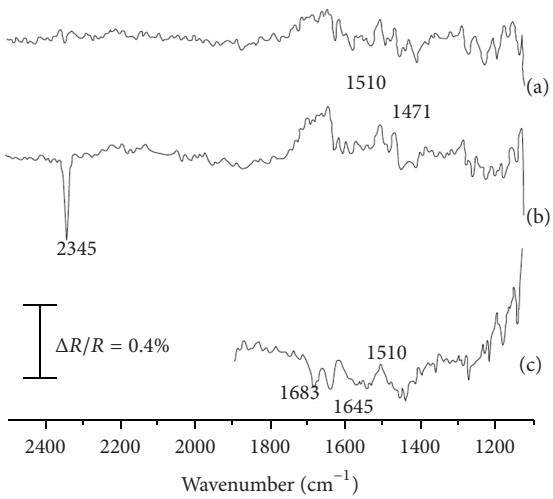

FIGURE 5: FTIR spectra for a Pt electrode in a 1 M $HClO_4$ + 5×10^{-3} M *o*-AP solution. (a) Sample potential: 0.8 V, (b) sample potential: 1.0 V, and (c) spectrum obtained at 0.9 V in deuterated water. P-polarized light, 100 interferograms. Reference potential: 0.4 V [49].

A positive band at 1374 cm^{-1} was also observed and was assigned to the C–N stretching of the secondary aromatic amine that also disappeared at 0.7 V. Two negative bands were observed at 1558 cm^{-1} and were associated with the C=N stretching vibration of the imine group that is produced at higher potentials in the oxidation of phenoxazine. As bands corresponding to proposed alternative structures, where the polymer remains linear and the –OH groups are free and could be oxidized to *ortho*-quinonimines (Figure 3), were not observed in [49], it was concluded that the most probable structure of the polymer formed in the oxidation of *o*-AP contains the phenoxazine unit as the main constituent of its structure. Theoretical calculations carried out in [49] seem to confirm that the polymer obtained by electro-oxidation of *o*-AP has a ladder structure built by phenoxazine units. In this regard, the electronic density of *o*-AP was calculated in [49] by employing the semiempirical self-consistent field method (AMI). It was found that *o*-AP has a high electron density in the *para* position with respect to the $–NH_2$ group. Therefore, dimers could be formed through attack of the cation radical at that position. The dimer of *o*-AP has a higher electron density in the *para* position with respect to the –OH group, allowing closing of the phenoxazine ring (Figures 3 and 6).

The electrochemical formation of POAP was also described by Ortega [2]. Ortega focussed his attention on the monomer purification before electropolymerization. *O*-AP (purum 90%) was purified by recrystallizing it three times in ethyl acetate. The very pale white plates were dried in a warm water bath under vacuum to eliminate residual solvent. The monomer was stored in a desiccator under vacuum until required. MNR, IR, and C^{13} spectra were recorded in order to ensure the absence of contaminant oxidation species in the monomer. The comparison of voltammograms obtained by Ortega with those shown by Barbero et al. in [1] for 3APZ allowed Ortega to conclude that the coupling of 3APZ units to form the polymer is the process that occurs during the propagation of the polymeric chains.

With the aim of discerning whether 2-aminophenoxazin-3-one (3APZ) is the repetitive unit of POAP films or is incorporated into the film structure during its synthesis, a spectroscopic characterization of soluble products in an electrolyzed *o*-AP solution was carried out by Gonçalves and coworkers in [4]. Drastic optical changes were noted after applying a constant potential of 0.85 V (*versus* RHE) on a Pt wire immersed in a spectrophotometer cell containing an *o*-AP solution. Each deconvoluted UV-Vis spectrum of this solution led to two or three main absorption bands, depending on the time at which the measurement was taken. For comparison purposes, the spectra of the electrolyzed solution were compared with that of 3APZ. While the electrolyzed solution presented an absorption band at 400 nm, a well-defined band at 460–470 nm characterized 3APZ. The absorption band at 400 nm was assigned to quinone intermediates continuously formed during electrolysis (benzoquinone, benzoquinone-monoimine, and benzoquinone-diimine). Although isolation of intermediates failed, 2-aminophenoxazin-3-one (3APZ) was identified in [4] as the final product after extraction from the electrolyzed *o*-AP solution. This assignment was supported by not only UV-visible spectroscopy, but also by IR and ^{1}H-NMR spectroscopy and elemental analysis. In order to establish whether 3APZ undergoes any polymerization process, Pt and GC electrodes were cycled in a medium containing chemically synthesized 3APZ. Voltammetric results obtained in [4] indicate that 3APZ does not undergo any polymerization process. Then, in another experiment carried out in [4], chemically prepared 3APZ was dissolved in acetone and dropped on Pt and GC electrodes in order to prepare 3APZ films. In this case, a single well-defined redox process was observed in the voltammograms on both Pt and GC electrodes. Due to similarities between redox responses of POAP-modified Pt and GC electrodes and 3APZ-modified Pt and GC electrodes, an infrared study was also performed in [4] to establish whether 3APZ is the repetitive unit of POAP films, or is incorporated into the film structure, or POAP films and modified electrodes cycled in a 3APZ medium may present similar redox responses. The IR spectra of the chemically synthesized APZ, the soluble product extracted after electrolysis of *o*-AP solution, a POAP film and phenoxazine were compared in [4] (Figures 8(a), 8(b), 8(c), and 8(d), resp.). Similar IR signals for the extracted product and 3APZ indicated that they are the same materials. In this regard, Figures 8(a) and 8(b) present similar signals (the main coincident peaks were marked with dots) at 3300–3500 cm^{-1} due to the presence of NH_2 groups, and at about 1600 cm^{-1} due to the axial stretching of the C=O groups in the APZ structure. However, POAP presents a different spectrum (Figure 8(c)), and, then, different structures were proposed in [4] for POAP films and APZ. Common peaks are observed in Figures 8(c) and 8(d) at 1070 and 1111 cm^{-1}, respectively, which were assigned to the stretching of the C–O–C linkages. Also, the peaks in the region 1400–1600 cm^{-1} were attributed to the stretching of C–H and C–C groups. Then, similarities were found between the POAP film spectrum and that of

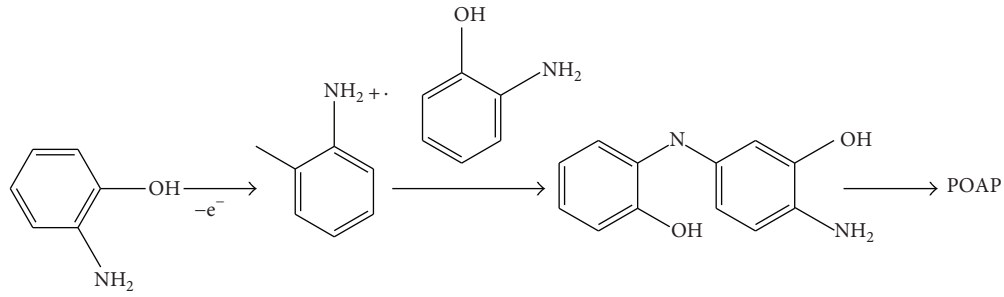

Figure 6: Scheme of *o*-AP oxidation to produce POAP [49].

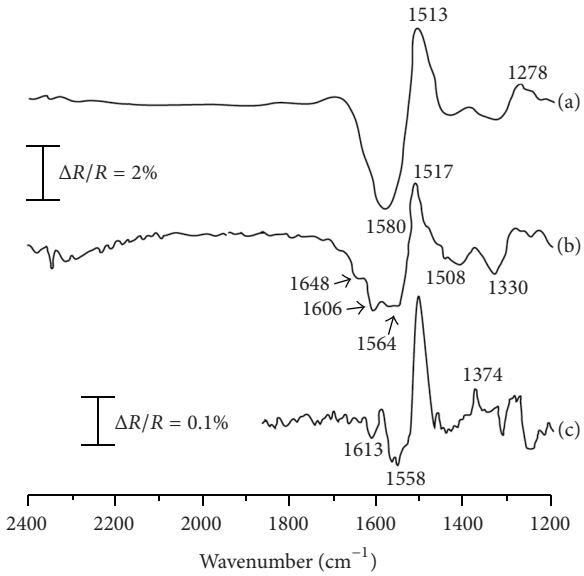

Figure 7: FTIR spectra for a Pt electrode covered with POAP in 1 M $HClO_4$ solution in (a) water and (b) deuterated water. Sample potential: 0.7 V and reference potential: 0.1 V. P-polarized light, 100 interferograms. (c) FTIR spectrum obtained for a Pt electrode in 1 M $HClO_4 + 5 \times 10^{-4}$ phenoxazine solution in deuterated water. Sample potential: 0.7 V and reference potential: 0.4 V. P-polarized light, 100 interferograms [49].

phenoxazine. It was concluded in [4] that despite the fact that POAP films may present phenoxazine units and then similar redox responses can be expected for POAP films and 3APZ modified electrodes, 3APZ does not polymerize.

Gonçalves and co-workers [4] postulate that the electrochemical oxidation of *o*-AP consists of a first oxidation step involving a two-electron transfer to form radical cations followed by chemical couplings of a radical cation-radical cation or radical-monomer species (E(CE)) mechanism to form a ladder polymer with phenoxazine units.

However, radical cations can also react quickly near the electrode surface, and after the first step involving two electrons, soluble products are easily formed by hydrolysis (Figure 9). Thus, besides a film with a ladder structure, Gonçalves and co-workers propose that oxidation of *o*-AP can produce intermediate benzoquinone monoamine after successive cycling. Particularly, under less controlled conditions such as at higher final potentials and lower scan rates, monoamines can react with neutral *o*-AP giving an intermediate (2-amino-*o*-indophenol) prior to cyclization to 3APZ. The low solubility of POAP films was attributed to the stiffness of the ladder phenoxazine backbone, which also seems to justify the low conductivity of POAP (10^{-7} S cm^{-1}) as compared with that of PANI (1 S cm^{-1}).

Kunimura and co-workers [6] prepared POAP on basal-plane pyrolytic graphite (BPG) and In-Sn oxide conducting glass (ITO) by electro-oxidative polymerization of *o*-AP. The IR absorption spectrum of the oxidized form of POAP was compared with those of *o*-AP and phenoxazine (Figures 10(a), 10(b), and 10(c), resp.). Although common absorption peaks for the three compounds were observed in [6], other peaks were not common. The absorption peaks due to the N–H stretching vibrations of the imino group of the POAP film and phenoxazine were observed at 3420 cm^{-1}, while two absorption peaks corresponding to the N–H stretching vibrations of the amino groups of *o*-AP were observed, as expected, at 3340 and 3420 cm^{-1}. The presence of a relatively strong absorption peak at around 3420 cm^{-1} was considered as an indication that POAP does not possess a completely ring-closed structure, as proposed in [1]. In this regard, a partially ring-opened structure as that shown in Figure 11 and/or a relatively low degree of polymerization of *o*-AP were proposed in [6].

The absorption peaks ascribable to the stretching vibrations of C–N bonds were observed for POAP at 1250 and 1310 cm^{-1}. Similar peaks were observed for *o*-AP and phenoxazine. The peak at 1645 cm^{-1} in the POAP spectrum was assigned to the stretching of the C=N bonds present in a ladder polymer with phenoxazine rings. The absorption peaks at 1050 cm^{-1} and 1235 cm^{-1}, which are characteristic of the C–O–C stretching vibration, were observed for POAP and phenoxazine, but not for *o*-AP. Peaks at 760, 850, and 935 cm^{-1} for POAP were assigned to 1,2-disubstituted, 1,2,4-trisubstituted, and/or 1,2,4,5-tetrasubstituted benzene structures, respectively. All these structures were considered to be possible for POAP. Furthermore, from the fact that

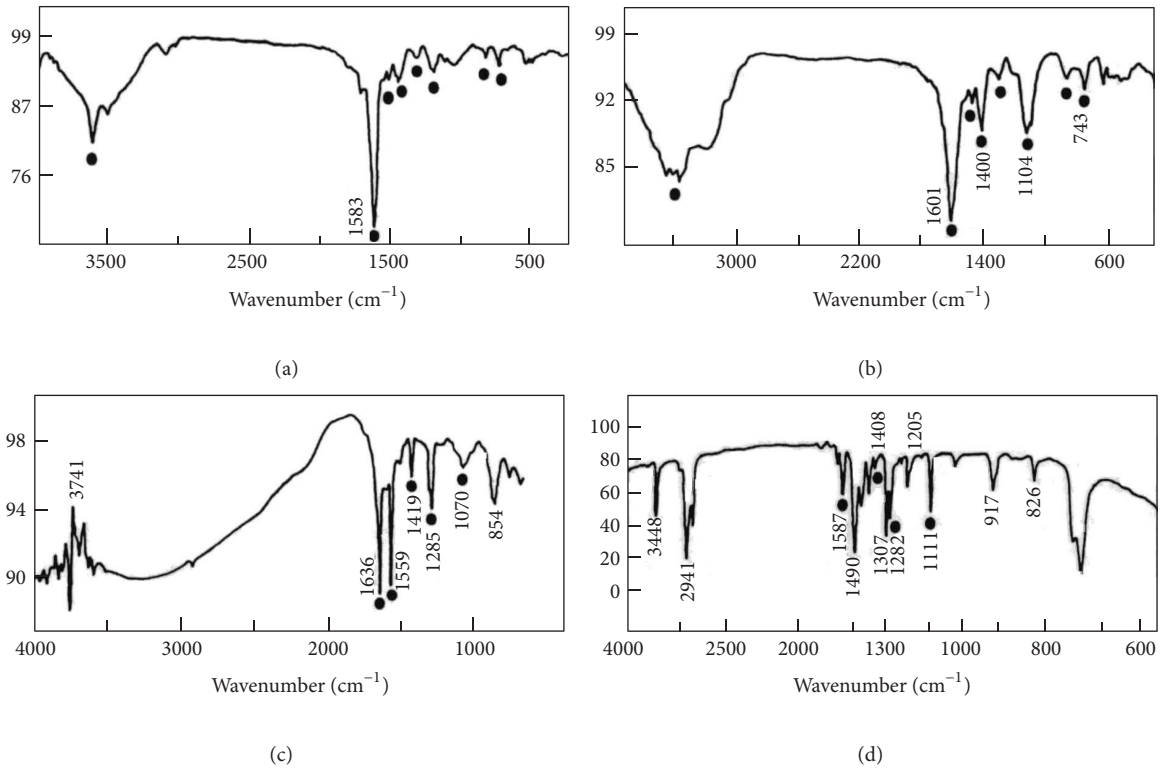

Figure 8: Infrared spectra of (a) extracted product from electrolyzed *o*-AP solution; (b) chemically synthesized 2-aminophenoxazin-3-one (3APZ); (c) POAP film (prepared on Pt by cyclic voltammetry, 400 cycles); and (d) model compound (phenoxazine) [4].

the absorption peak, which is assigned to the stretching vibration of the C=O bonds of aromatic keto groups, was observed at 1670 cm^{-1}, not only the partially ring-opened structure shown in Figure 11, but also the structure shown in Figure 12, which was assumed to proceed from a polymerization via C–N=C bonds, was proposed for POAP in [6].

Zhang et al. [7] studied the chemical and electrochemical synthesis of POAP employing spectroscopic measurements. POAP was chemically synthesized by treatment of an acid solution of *o*-AP with $CuCl_2$, and the oxidative polymerization was followed by UV-Vis spectroscopy. Prior to the addition of $CuCl_2$, two absorption peaks were found on the monomer solution spectra at 258 and 460 nm and were assigned to the $\pi \rightarrow \pi^*$ transition of the aromatic structure (benzene structure) and the oxidized form of *o*-AP, respectively. A new absorption peak at 410 nm developed after the addition of Cu(II), and its intensity increased with time at the expense of the peak at 460 nm. The 410 nm peak, which is common among PANI-like structures, was assigned to the radical cation (oxidized form) of POAP. The solid polymer synthesized in [7] was also examined by X-ray photoelectron spectroscopy (XPS). It was noticed that the C1s, N1s, and O1s spectral features were similar to those reported for electrochemically prepared POAP in other papers [50]. The carbon spectrum was deconvoluted to estimate the extent of carbon involved in C–C, C–N, and C=O bonds. A ratio of 3 : 2 : 1, indicating a good degree of polymerization, was obtained. A Cu2*p* peak was also observed at the binding energy of 932.2 eV, suggesting the presence of copper remnant in the polymer. Experimental results presented in [7] substantiate the feasibility of chemical synthesis of POAP by the anodic oxidation of *o*-AP by the Cu(II)/Cu(I) redox couple.

The electrochemical synthesis of POAP was performed in [7] on GC electrodes from a 1 M SO_4H_2 + 0.5 M Na_2SO_4 + 0.05 M *o*-AP solution, and it was studied by cyclic voltammetry and reflectance changes in the Vis spectrum region and Raman spectroscopy. The evolution of the cyclic voltammogram during polymerization of *o*-AP within the potential range comprised between −0.2 V and 1.0 V (SCE) is described in detail in [7]. Three redox pairs were observed. The most negative redox pair was observed at around 0–0.15 V, and it was the only noticeable feature in the cyclic voltammogram of POAP in an acid medium without the monomer. The other two redox processes were observed at around 0.2–0.4 V and 0.5–0.7 V, respectively. While the redox pair at around 0–0.15 V was attributed to the redox reactions of *o*-AP polymers and/or oligomers, the other two more positive peak systems were associated with the oxidation of *o*-AP to the radical cation ($OAP^{\bullet+}$) and its further oxidation to the dication, respectively. While the peaks of the redox pair at 0–0.15 V increased steadily with an increasing number of scans, showing the gradual but continual formation of electroactive POAP, the peaks of the other two redox pairs decreased. The flattening of the two more positive peak systems was attributed to a limitation

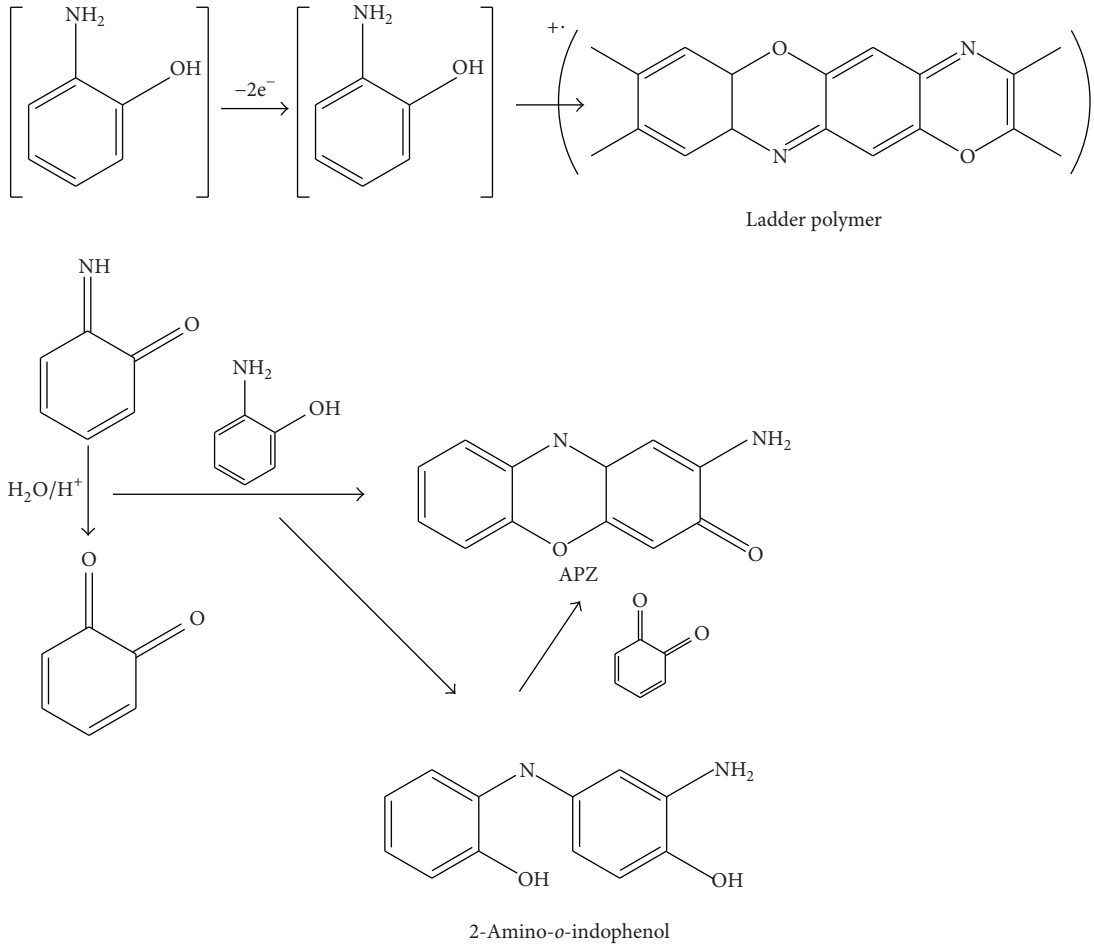

Figure 9: Mechanism of *o*-AP electro-oxidation in aqueous acidic medium [4].

to *o*-AP diffusion during the polymerization process. The scarce formation of the radical cation (polaron) and dication (bipolaron) during the polymerization was associated with restricted charge-transport processes and electron delocalization effects along a partly cross-linked polymer chain. Zhang et al. compare the electropolymerization process of *o*-AP with that of aniline in [7]. In this regard, they remarked that this reaction pathway is markedly different from the polymerization of aniline because in PANI deposition the oxidized monomers (nitrenium cations), which are reactive towards the phenazine rings in aromatic electrophilic substitutions, are only produced at high potential and low aniline concentration. As a result, PANI polymers of a different structure from the normal variant are formed under such conditions. In contrast, the deposition of POAP proceeds mainly through the direct oxidation of the monomer. Also, the authors in [7] remark that the easy oxidation of *o*-AP is in contrast to that of other aniline derivatives such as metanilic acid. The presence of the electron-donating OH group in *o*-AP facilitates monomer oxidation, whereas metanilic acid is difficult to oxidize because of the presence of an electron-withdrawing SO_3 group. In this case, aniline must be added to produce sufficient dications to sustain polymer growth. With regard to reflectance measurements carried out in [7], the wavelength dependence of the relative reflectance $\Delta R/R$ change for a POAP film electrochemically deposited on Pt when it is polarized at various potentials was analyzed. A broad absorption band extending from 410 nm to 532 nm was observed for polarization within the range 0.1 V–1.1 V (SCE). The band intensity increased with increasing potential, turning the film dark brown. In addition, a slight blue shift, simultaneously with the intensity increase, was noted. The absorption band was assigned to the formation of radical cations at POAP, as the polymer matrix becomes oxidized. It is indicated in [7] that this behaviour is similar to that of PANI, for which the first oxidation of the polymer to a radical cationic species also produces an absorption band near 440 nm. Besides, in the same way as for PANI, the blue shift in the absorption band with increasing potential suggests that the polymer was more extensively oxidized and subsequently contained a larger fraction of the radical cationic species. Zhang et al. [7] also apply Raman spectroscopy to elucidate the POAP structure. These authors confirm that the POAP matrix contains alternating oxidized (quinonoid) and reduced (N-phenyl-*p*-phenylenediamine) repeating units (Figure 13). The similarity between

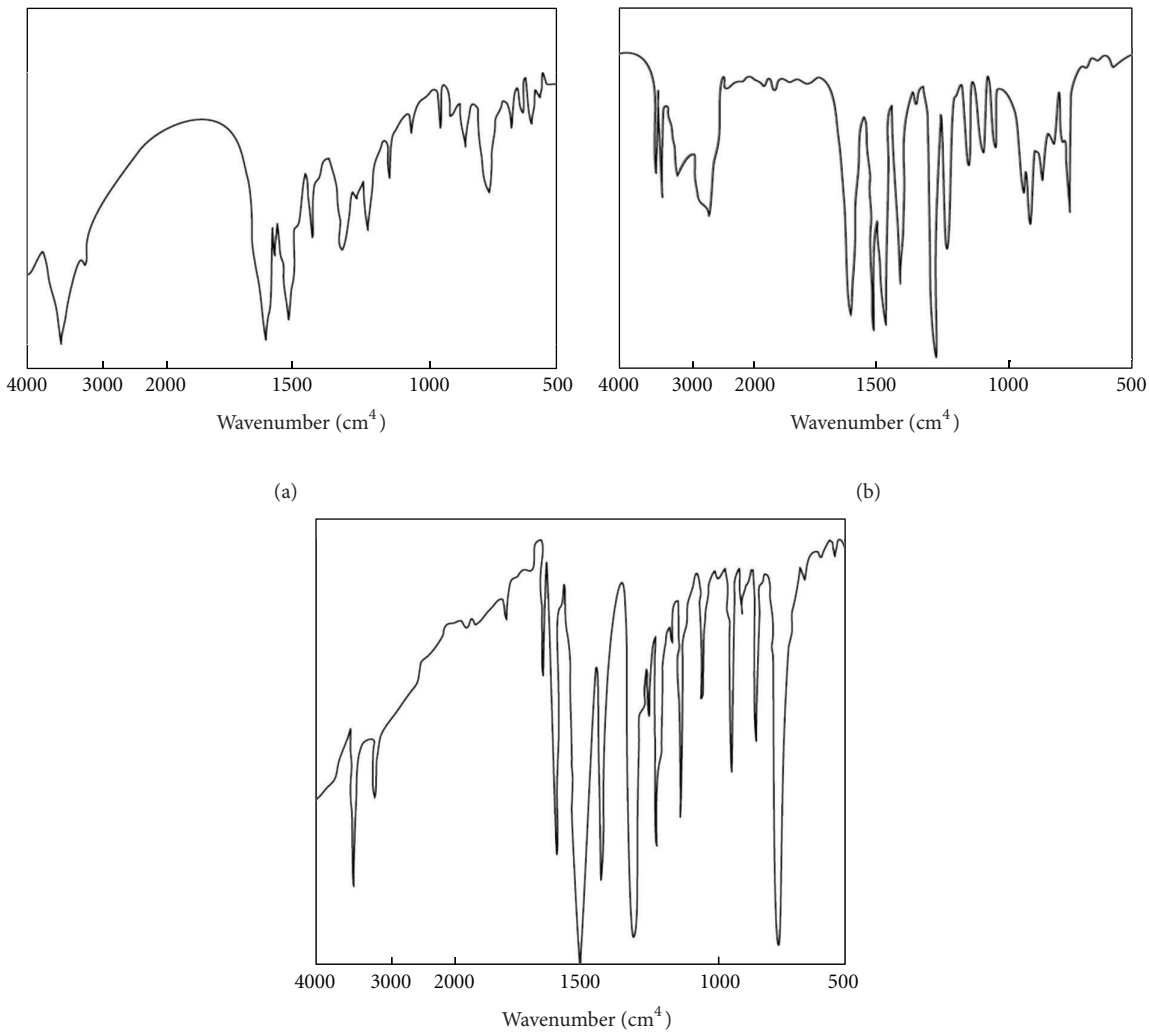

Figure 10: IR absorption spectra of (a) a POAP film (oxidized form), (b) *ortho*-aminophenol (*o*-AP), and (c) phenoxazine. The POAP film was prepared on BPG [6].

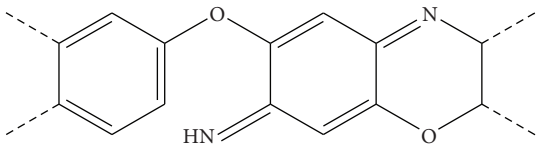

Figure 11: Partially ring-opened structure of POAP [6].

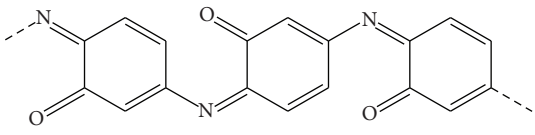

Figure 12: Partially hydrolyzed structure of POAP [6].

the structure shown in Figure 13 and that of PANI shown in [51] is also pointed out by the authors in [7]. Then, in [7], the redox reaction of POAP was assumed to be an internal conversion between the oxidized and reduced units that can be represented by the stoichiometry shown in Figure 14. Polarization of the polymer at a potential more positive than 0.1 V (SCE) transforms the polymer into the quinonoid form, whereas the reduced units predominate only at negative potentials. According to the authors in [7], an increase of the potential increases the extent of oxidation in the polymer, but Raman spectroscopy indicates that the oxidation is not complete even at 0.5–0.6 V (SCE). Then, the broad absorption band extending from 410 nm to 532 nm in the reflectance change described previously was assigned to the contribution of $\pi \rightarrow \pi^*$ transitions from both oxidized (quinonoid) and reduced (N-phenyl-*p*-phenylenediamine) units. The absence of differentiable

absorption peaks within the wavelength range of interest was considered to indicate that the two $\pi \rightarrow \pi^*$ transitions occur at very close frequencies. According to Barbero et al. [52], the separation is about 80 nm. Again, the authors indicate that this is in marked contrast with PANI, for which the absorption peaks of oxidized and reduced units are well separated over a wavelength of 200 nm [53]. The increase of the total integrated absorption intensity with oxidation observed in [7] indicated that the oxidized units had higher specific absorbance values than the reduced units. Subsequently, a reduced POAP film was observed to be semitransparent with a tint of light brown colour, whereas a more oxidized film was opaque with a tint of darker brown colour. The main conclusions derived from UV and Raman measurements in [7] are (i) POAP growth proceeds mainly through the reactions between the growing polymer and oxidized monomer units, and subsequent cyclization of the functional units in the polymer leads to a ladder structure; (ii) the POAP matrix consists of both oxidized (quinonoid) and reduced (N-phenyl-*p*-phenylenediamine) monomer repeating units; and (iii) the easy formation of radical cations from the oxidation of *o*-AP differentiates the electropolymerization of *o*-AP from that of aniline and its other derivatives such as metanilic acid.

The POAP structure proposed in [7] was verified by Zhang and co-workers in another work [8]. POAP films were synthesized on GC and Pt electrodes from a solution containing 0.05 M *o*-AP in a mixture of 1 M H_2SO_4 and 0.5 M Na_2SO_4 to study the oxidation process of POAP deposits of different thickness. The potential was scanned from −0.2 V to 0.8 V (SCE) at 100 mV s^{-1} for different numbers of cycles (N). The extent of the oxidation of the polymer films was investigated at the open-circuit potential of POAP. The synthesis conditions employed in [8] allowed the authors to propose the same POAP structure formulated in [7] (Figure 13). The relative proportions of alternating oxidized (quinonediimine) and reduced (phenylenediamine) repeating units were considered to be dependent on the oxidation state of the polymer. Although the polymer synthesized in [8] corresponds to the reduced state ($E = -0.2$ V) of POAP, it was observed that it was readily oxidized by dissolved oxygen in the electrolyte and the extension of the oxidation depended on the film thickness.

Thick films are more difficult to oxidize and often result in a mixture of reduced and oxidized forms. With the diffusion of oxygen impeded by the increase of the film thickness, oxidation of thick POAP films was confined mostly to the polymer exterior. The structure of POAP shown in Figure 13 also allowed the authors in [8] to explain the interaction of the polymer with metal cations. In this regard, it was observed that when POAP films deposited from 150 voltammetric cycles are equilibrated in a 0.1 M $AgNO_3$ solution for 30 min, the films capture silver cations. The cation capture process was attributed to the simultaneous presence of hydroxyl and amino groups of the polymeric backbone of POAP, in which the lone pair electrons are available to coordinate with metal cations. The interaction of POAP with silver ions ranged from redox reactions, in which cations were reduced to the metallic form, to a partial charge transfer between the metal and the polymer resulting in the formation of a metal-polymer complex. These two types of interactions predominate in thick films ($N = 120$) and thin films ($N = 1$), respectively. Films of moderate thickness ($N = 20$) exhibited intermediate behaviour. The Ag^+-POAP complex synthesized in [8] was also compared with that of Ag-PANI [54]. It is indicated that the Ag^+-POAP complex presents an improved stability over that of Ag^+-PANI due to the cooperative action of the oxygen atom in the POAP chemical structure. Besides, the redox reaction of silver is within the range of the POAP redox reaction, and, then, changes of POAP conductivity were not significant during the redox reactions of the POAP-Ag^+ complex. This was very different from the situation of the Ag^+-PANI complex, where the redox switching of PANI between the insulating state of leucoemeraldine and the conducting state of emeraldine has substantial influence on the voltammetric response of silver redox behaviour. Also, it has also been demonstrated in [8] that POAP is more resistant than PANI to electrochemical degradation and can capture silver four times more than PANI. The POAP-Ag(I) complex also exhibits electrocatalytic activity in dissolved oxygen reduction. However, it was observed that silver can be released from the complex upon acidification of the nitrogen and oxygen atoms or upon application of a sufficient positive potential.

The 1,4-substituted molecular structure of POAP proposed by Zhang et al. [7, 8] (Figure 13) also seems to be consistent with the electrochemical response of POAP films to ferric cation in solution [55, 56]. It was reported in [56] that POAP films obtained on ITO electrodes by electropolymerization of *o*-aminophenol (0.1 M) in a 0.1 M H_2SO_4 aqueous solution, after being soaked in a ferric cation solution, can act as potentiometric Fe(III) ion sensors. In this regard, POAP films immediately synthesized in [56] showed the IR spectra that correspond to a 1,4-substituted structure. When these POAP films are soaked for 24 h in a 0.1 M H_2SO_4 aqueous solution containing 50 mM $Fe_2(SO4)_3$, their XPS spectra show iron ion capture. The ferric cation capture process was attributed to the simultaneous presence of hydroxyl and amino groups of the polymeric backbone of POAP. After this cation capture process, the electrode potential of the POAP film was measured in various aqueous solutions containing Zn(II), Ni(II), Cu(II), Fe(II), and Fe(III) ions at different concentrations. The relationship between the electrode potential, E, and the logarithm of the concentration, C, in different solutions was recorded. The electrode showed no potential response to ion concentration for Zn(II), Ni(II), Cu(II), and Fe(II) ions. However, it showed a Nernstian potential response to Fe(III) ions with a slope −57 mV/log [Fe(III)]. The response time was less than 10 s, and the response was observed until [Fe(III)] = 10^{-4} M. The response to Fe(III) ions in solution was considered indicative of the presence of Fe(II) in the POAP film. The presence of Fe(II) in the film was explained considering that the captured Fe(III) ions are at least in part reduced to Fe(II) by the film. The potentiometric response was attributed to the electron transfer between Fe(II) ions in the film and Fe(III) ions in solution.

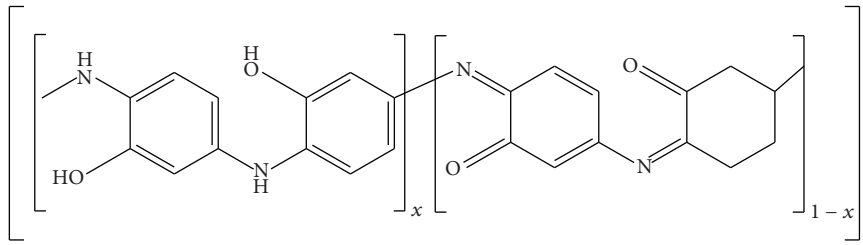

Figure 13: Structure of POAP as an alternating series of oxidized (quinonoid) and reduced (*N*-phenyl-*p*-phenylenediamine) repeating units. X is the mole fraction of reduced units in the polymer, and hence $x = 0$ and $x = 1$ correspond to a fully oxidized and reduced polymer molecule, respectively [7].

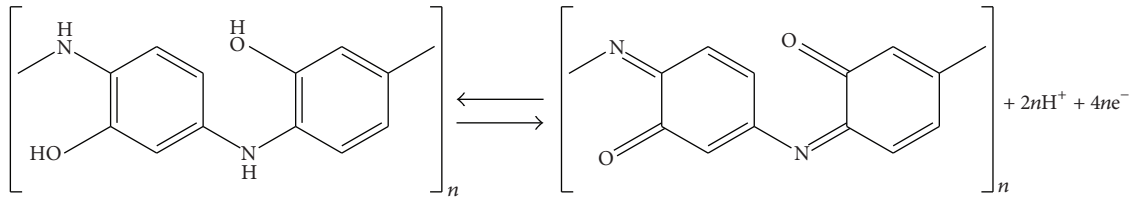

Figure 14: Stoichiometry of redox reactions of POAP film electrode [7].

3. Spectroscopic Studies of the Redox Process of POAP in Acid Medium

A spectroelectrochemical study of the redox process of POAP is reported in [57]. Absorbance changes in the wavelength region comprised between 300 nm and 800 nm, at different pH values and in the presence of different supporting electrolytes, were recorded and analyzed at different degrees of oxidation of POAP. Two types of experiments were carried out in [57]. (i) At a fixed wavelength, the electrode potential was swept at scan rates comprised between 0.005 and 0.03 V s^{-1}. (ii) At a fixed electrode potential, the wavelength was scanned between 300 nm and 800 nm.

Figure 15 shows the spectra of POAP films at different electrode potentials in the region where the film is electrochemically active ($-0.2\,\text{V} < E < 0.7\,\text{V}$ versus SCE). The absorbance of the film at the negative potential limit (−0.2 V) was attributed to the tail of the UV band related to the $\pi \rightarrow \pi^*$ transition of the basic aromatic structure of the phenoxazine units. A reaction scheme for the POAP redox switching, which also includes protonation reactions, is shown in [57] (Figure 16). The redox switching of POAP was interpreted in terms of the oxidation of amine groups to imine groups. As POAP was progressively oxidized, several changes in the spectral response were observed (Figure 17): (i) an absorbance decrease in the wavelength region about 340 nm; (ii) a broad maximum developed at 450 nm; and (iii) in the region of $\lambda > 750$ nm, the absorbance first increases with the potential up to $E = 0.1$ V, and, then, for $E > 0.1$ V, the absorbance decreases. While the decrease of the absorbance at $\lambda = 340$ nm, as the potential increases in the positive direction, was attributed to the disappearance of the reduced form of POAP, the increase of the absorbance at $\lambda = 450$ nm was associated with the increase of the oxidized form with the potential scan. The broad band growing at 450 nm as the potential increases in the positive direction was assigned to the partially oxidized phenoxazine structure. At $\lambda = 750$ nm, the absorbance presents a maximum at $E = 0.15$ V, which was considered to be indicative of the existence of a transient species.

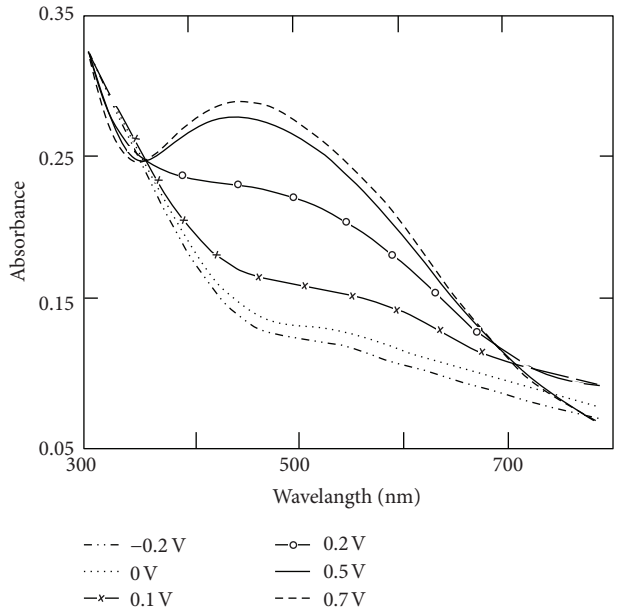

Figure 15: Absorbance as a function of wavelength at fixed electrode potentials, E, in 0.4 M $NaClO_4$ + 0.1 M $HClO_4$ [57].

Spectra of reduced ($E = -0.2$ V) and oxidized ($E = 0.7$ V) states of POAP were found to be dependent on pH. The absorbance difference $\Delta A = A_{ox} - A_{red}$ was analyzed in [57] and represented, at different pH values as a function of the wavelength while the polymer goes from the reduced state to

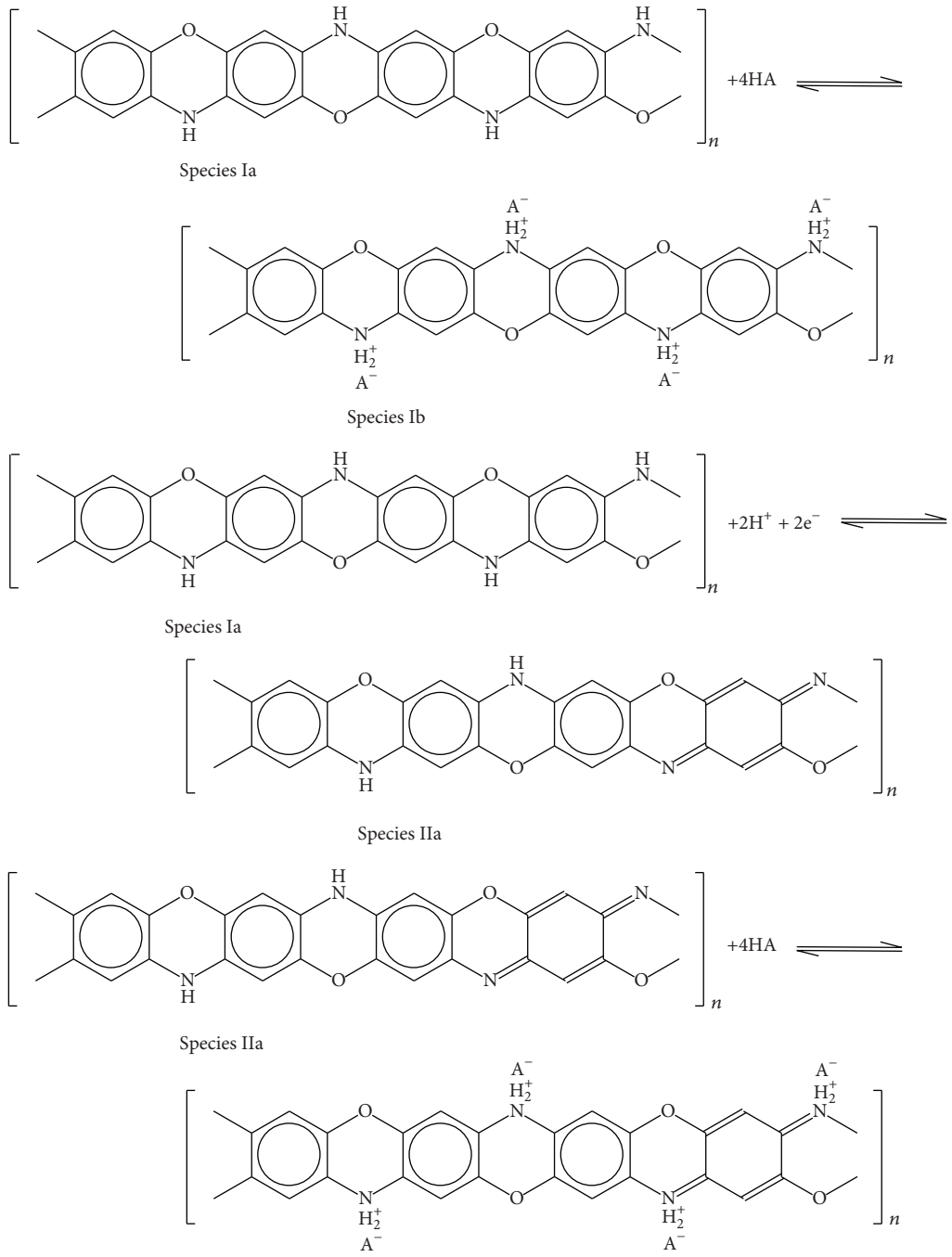

Figure 16: Reaction scheme of the POAP redox switching proposed in [6, 14, 57] including the protonation equilibria of the oxidized (species II) and reduced (species I) species.

the oxidized one. The observed increase in the ΔA difference in the UV region was associated with the conversion of one protonated amino group to a nonprotonated imino group. It was concluded in [57] that as the pH increases, the reduction of the oxidized species becomes progressively hindered and consequently the amount of oxidizable species available in the film decreases. Experiments carried out in [57] in the presence of different anions (perchlorate, sulphate, and benzenesulphonate) at pH 1 showed that the absorbance with potential at 440 nm decreases in the sequence ClO_4^- > HSO_4^- > benzenesulphonate. The transient response at 750 nm (Figure 17) was also dependent on the nature of the anion of the supporting electrolyte, thus, for benzenesulpHonate, the change was smaller than for perchlorate and bisulphate.

Raman spectroscopy and voltammetry were combined to identify structural changes during the redox process of POAP [58]. Voltammetric measurements at different perchloric acid

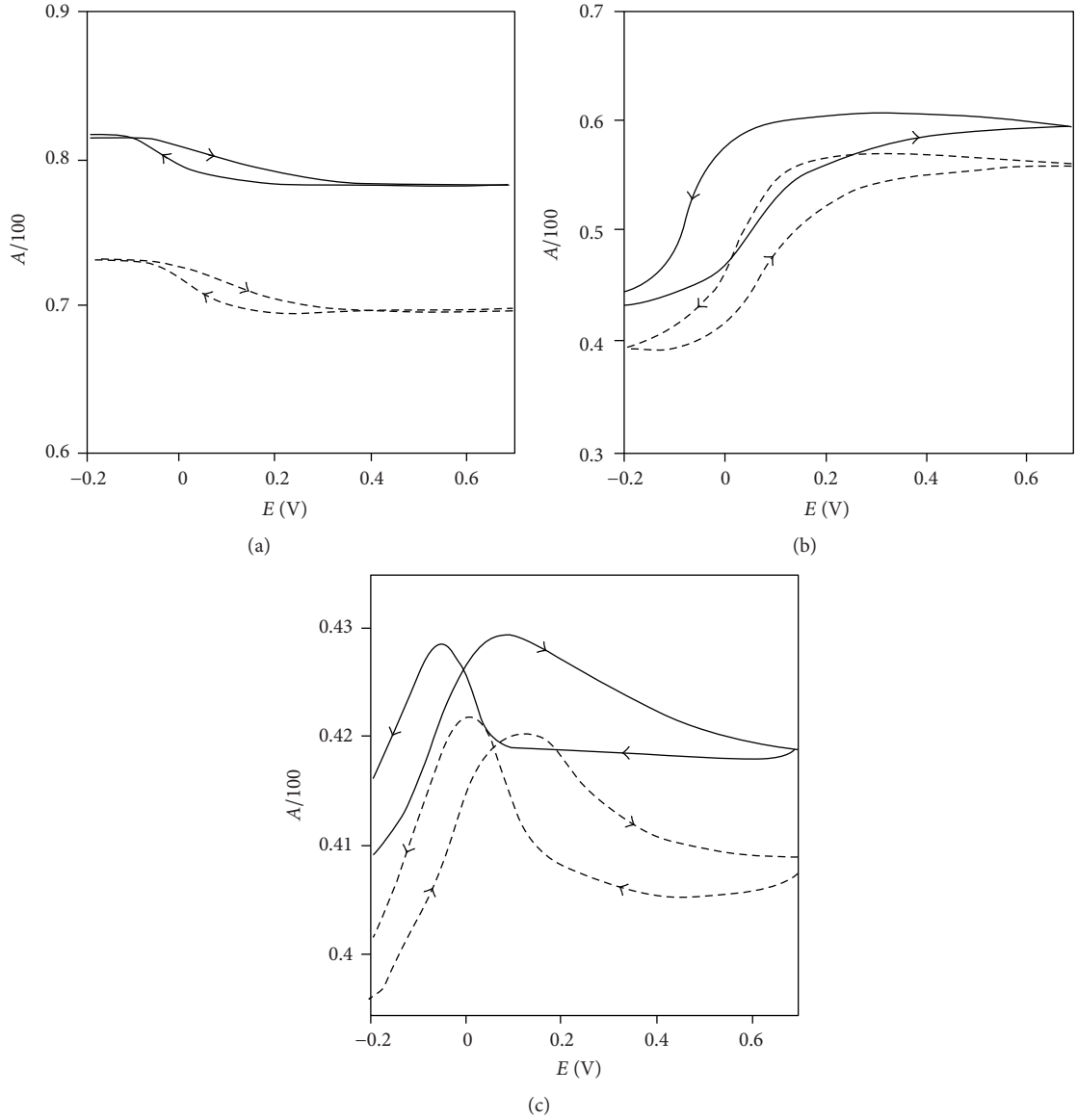

Figure 17: Absorbance as a function of potential at fixed λ values in $NaClO_4$ + $HClO_4$ at different pH values: (a) 340 nm, (b) 450 nm, and (c) 750 nm. The arrows indicate the potential scan direction: (- - - -) pH = 1.0 and (—) pH = 1.5. Sweep rate 0.01 V s^{-1} [57].

concentrations carried out in [58] revealed the existence of two redox processes for POAP films. The different bands of POAP extracted from an in situ Raman spectrum acquired at 0.1 V are listed in Table 4.

Bands at 1593, 1474, 1390, and 1160 cm^{-1} were associated with quinoid groups, while bands at 1520 and 576 cm^{-1} were assigned to aromatic rings. The band at 1638 cm^{-1} was attributed to –C=N– in quinonimine units. The intensity of some of these bands was found to be dependent on the applied potential. The behaviour of the bands with the applied potential shows that when the potential increases, the band at 1474 cm^{-1} increases and the band at 1638 cm^{-1} also increases until a potential of about 0.2 V and thereafter it diminishes. The fitting of both bands by Lorentz curves allowed quantifying the evolution with the potential of the corresponding species associated with these bands. The behaviour of the band at 1638 cm^{-1} was attributed to a typical intermediate species. The existence of intermediate species was explained on the basis of an oxidation process that occurs through two consecutive reactions from the totally reduced phenoxazine form to the completely oxidized one, through a charged species, which was considered to be a cation radical. Since POAP has a conductivity maximum at about 0.04 V (SCE), the intermediate species was related to the polymer conductivity. The behaviour of the integrated Raman intensity of the band at 1638 cm^{-1} was considered to be similar to that of the band at 750 nm observed in the absorbance versus potential dependence in the UV-Vis region reported in [57]. As the maxima of absorbance of both bands (750 nm [57] and 1638 cm^{-1}) appear approximately at the same

Table 4: Vibration modes observed by Raman spectroscopy in POAP-modified Au electrodes at 0.1 V in 1 M $HClO_4$ [58].

Wavenumber/cm^{-1}	Vibration modes
1638	–C=N– stretching of quinonimine units
1593	>C=C< stretching of quinoid units or $N–H^+$ deformation vibration on secondary amines
1520	–C=C– stretching in the aromatic ring
1474	–C=N– stretching of quinoid units
1390	C–C stretching of quinoid units
1328	$>C–N^{\bullet+}–$ stretching
1160	C–H bending in plane
925	Perchlorate vibration band
576	Ring deformation of benzenoid units

Table 5: Vibrational bands in Raman spibrational bands in Raman spectrectra (λ_0 = 647.1 nm) for a POAP film in a 0.5 M H_2SO_4 solution [9].

Wavenumber/cm^{-1}	Description
1645	C=N stretching of quinonimine units
1598	C=C stretching of quinoid units
1522	C=C stretching in the aromatic ring
1472	C=N stretching of quinoid units
1402	$C–N^{\bullet+}$ stretching of radical semiquinone
1330	$C–N^{\bullet+}$ stretching
1170	C–H bending in plane
982 and 1050	Sulfate modes
578	Ring deformation of benzenoid units

potential, this fact was considered to be indicative of the existence of two redox processes in the oxidation of POAP. A redox mechanism of POAP was proposed in [58] where the first step mainly involves the anion exchange, whereas in the second step the insertion/expulsion of protons is produced (Figure 18).

Evidence about the existence of cation radical species during the redox conversion of POAP was also reported by Ortega [2]. Ortega studied the conducting potential range of POAP by employing cyclic voltammetry and electron spin resonance (ESR) measurements. POAP films deposited on a Pt electrode were introduced into a solution at pH 0.9, which was free of monomer, and, then, ESR spectra were recorded at different potentials, scanning forwards and backwards from −0.250 to 0.55 V (Ag/AgCl). Figure 19 shows a typical signal at negative potentials, which starts decreasing until it reaches a very small value at 0.55 V. The maximum in ESR spectra occurs in the potential ranging from −0.24 to approximately 0.0 V (SCE). The decrease and further absence of a detectable ESR signal at potentials higher than 0.55 V were attributed to a combination of radicals to give rise to dication species, which are not ESR active because of their paired spin. Ortega concludes that at high positive potential values, the creation of bipolarons by a combination of polarons is possible at POAP films.

Shah and Holze [9] investigated the potentiostatic electrochemical polymerization of *o*-AP at different electrode potentials (E = 0.7 V; 0.8 V and 0.9 V versus SCE, resp.) with the aim of comparing the redox behaviours of the synthesized polymer by cyclic voltammetry and potentiostatatically. POAP films potentiostically synthesized at 0.7 V show two redox processes. The first redox process is centered at E = 0.16/0.15 V (SCE), while the second one is observed at E = 0.35/0.29 V. The contribution of the second redox process decreases as the potential applied during the electrosynthesis is increased. The voltammogram of POAP obtained at E = 0.90 V presents a somewhat intermediate behaviour between that of films obtained potentiostatically at E = 0.7 V and films potentiodynamically synthesized. In situ Raman spectra in the potential range comprised between the reduced (E = −0.2 V versus SCE) and the oxidized states (E = 0.5 V versus SCE) of POAP in 0.5 M H_2SO_4 solution for both potentiostatically and potentiodynamically synthesized POAP films were compared in [9]. The various bands together with their possible assignments are listed in Table 5.

The bands at 1598, 1472, and 1170 cm^{-1} were associated with quinoid groups, whereas the bands at 1522 and 578 cm^{-1} were attributed to benzoid rings. The band at 1330 cm^{-1} was assigned to semiquinone species with an intermediate structure between amines –C–NH– and imines –C=N– resulting in polarons. However, in [9] an additional band at 1402 cm^{-1} that was completely missing in the spectra reported in [58] was also observed. It was assigned to the radical semiquinone $C–N^{\bullet+}$ formed during the partial oxidation of N,N′-diphenyl-1,4-phenylenediamine. The bands located at 982 and 1050 cm^{-1} were assigned to internal modes of the sulphate anion of the electrolyte solution. It was observed in [9], that the intensity of some of the bands depends on the applied potential. For instance, the band located at 1170 cm^{-1} grew in intensity when shifting the potential up to E = 0.2 V, beyond this value it diminished with a further increase of potential. The dependence of the intensity of this band on the electrode potential was considered to be a characteristic feature of the oxidized form of POAP and was attributed to the CH bending vibrational mode of the quinoid-like rings formed during electro-oxidation. The bands in the frequency range 1300–1400 cm^{-1} were mainly associated with the stretching vibrations of charged $C{\sim}N^+$ segments (~denotes the bond intermediate between the single and double bonds).

Although the Raman features reported in [9] for potentiostatically and potentiodynamically synthesized POAP films were similar, marked differences with respect to the potential dependence of some bands were observed. A difference was observed particularly with respect to the potential dependence of the band around 1645 cm^{-1}. The intensity of this band sharply increased at 0.3 V and slowly decreased at more positive potentials for the POAP film synthesized

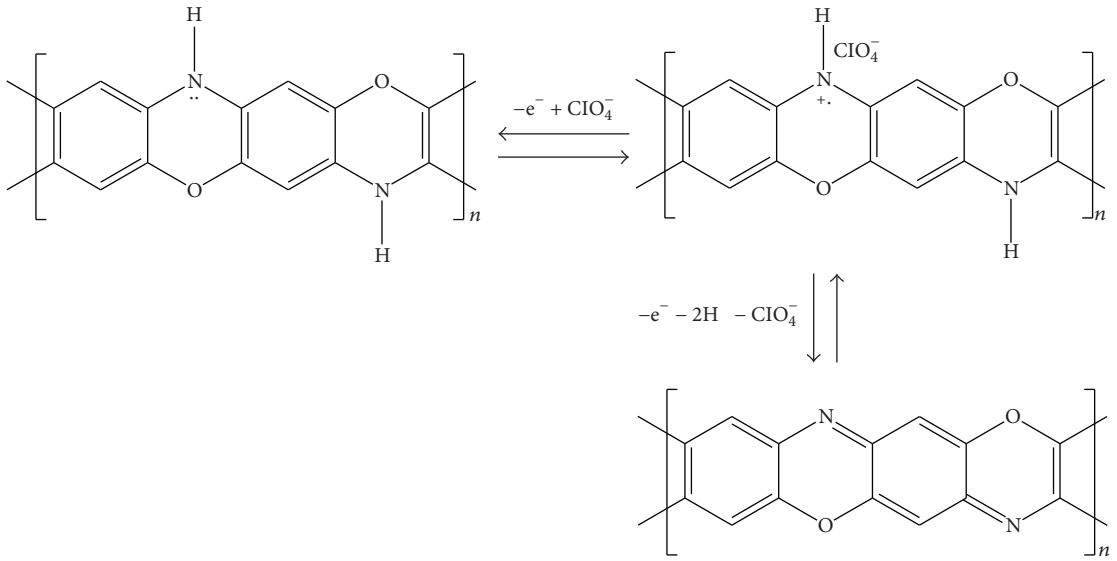

Figure 18: Reaction scheme for POAP oxidation in acid medium [58].

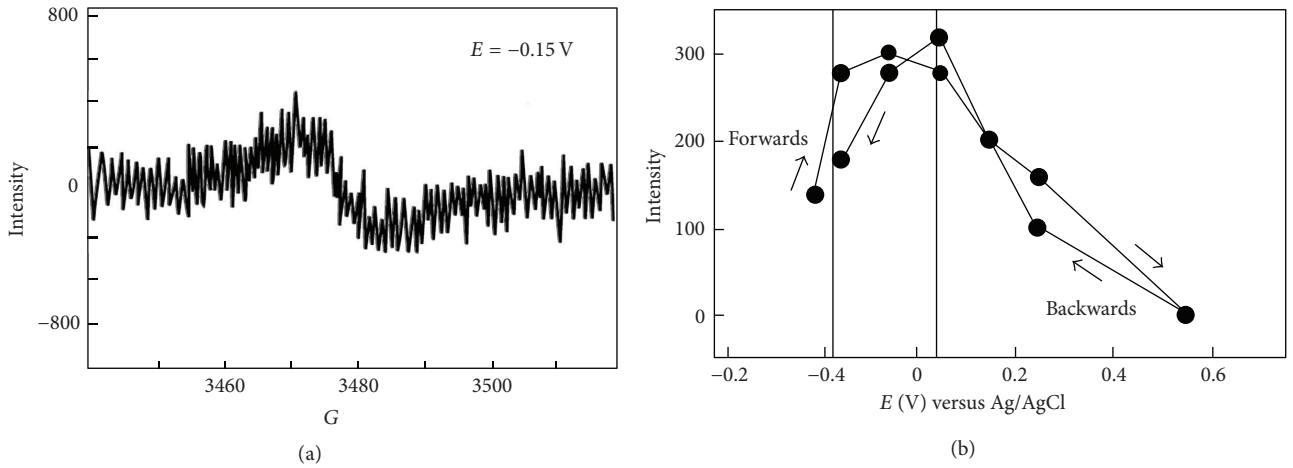

Figure 19: (a) Typical ESR spectrum of an 80 nm thick POAP film on Pt electrode at pH 0.9. Plot (b) illustrates the change in the ESR intensities as a function of potential. The maximum intensities are shown between the dotted straight lines [2].

potentiostatically. However, in the case of potentiodynamically prepared POAP, this band attained the intensity maximum at about $E = 0.2$ V. The band located at 1645 cm^{-1} was assigned to –C=N– in quinonimine units and was considered to correspond to the C–N–C bond of a heterocyclic six-membered ring structure arising from *ortho*-coupling rather than *para*-coupling during the electropolymerization, resulting in a ladder polymer. As this band did not disappear even at the highest applied potential, the oxidation of fully reduced POAP synthesised potentiostatically to fully oxidized POAP was assumed to proceed via an intermediate half-oxidized state. This assumption is supported by the fact that the maximum intensity of the band at 1645 cm^{-1} occurred at roughly middle potential between the two redox processes observed on the cyclic voltammograms of POAP shown in [9]. The effect was associated with the maximum of polaron concentration in the polymer. The increase of potential beyond the maximum intensity, which leads to the fully oxidized state of the polymer, was attributed to a lowering in the polaron concentration probably by coupling into bipolarons. Then, cyclic voltammetric and spectroelectrochemical results of potentiostatically prepared POAP films reported in [9] suggest the existence of charged intermediate species during the redox transformation of the film. The results support the oxidation scheme of POAP shown in Figure 20, which is based on the assumption that the incorporation of anions proceeds at less positive potentials and the expulsion of protons from the POAP polymer at more positive potentials. This oxidation process is assumed to proceed simultaneously for potentiodynamically prepared POAP films [58].

UV-Vis spectra of POAP films synthesized potentiostatically at different electrode potentials were also analyzed by Shah and Holtze [9]. Figures 21(a) and 21(b) show the UV-Vis spectra of a POAP film at different electrode potentials

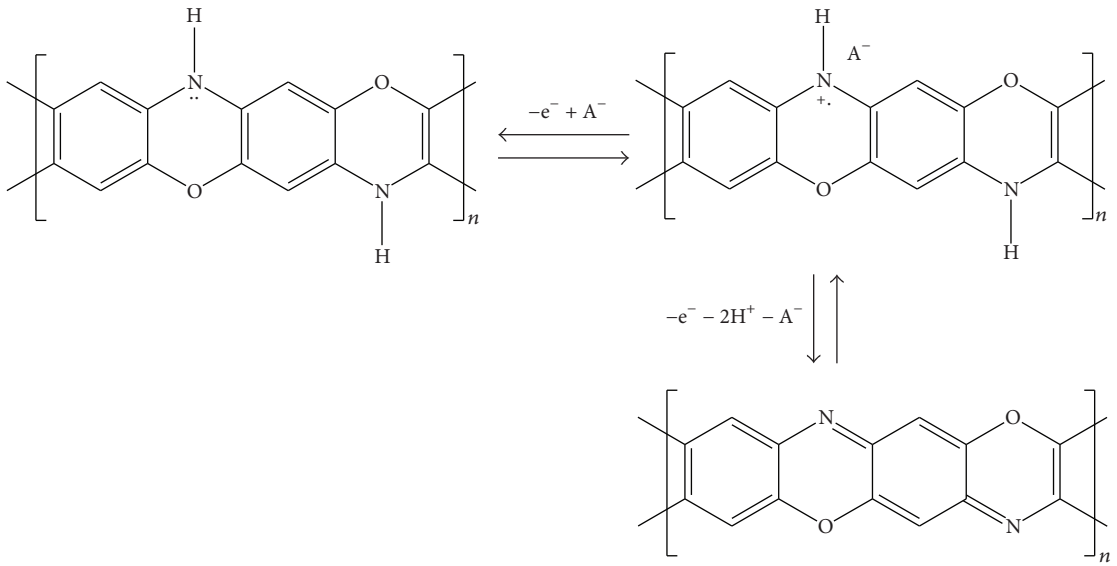

Figure 20: Reaction scheme for POAP oxidation in acid medium. POAP was potentiostatically synthesised [9].

within the range $-0.2\,\text{V} < E < 0.6\,\text{V}$ (SCE). Three absorption peaks located at $\lambda = 350$, 410, and 610 nm are observed, respectively. At $E = -0.2$, the polymer is in its reduced state and the corresponding spectra show an absorption band located at approximately $\lambda = 350\,\text{nm}$. This band was attributed to the phenoxazine structure. With increasing potential, the oxidation of POAP takes place, leading then to the formation of radical cations. It was observed that as the potential is increased from −0.2 V to 0.1 V, the intensity of the band at $\lambda = 350\,\text{nm}$ decreases, and also at 0.1 V, it is split into at least two bands. With further increase of the potential, the intensity of one of these bands diminishes, while the other one starts to shift to lower energies and changes into a broad maximum at around $\lambda = 410\,\text{nm}$. The absorption band at $\lambda = 610\,\text{nm}$ increases in intensity up to 0.2 V, and then it becomes nearly constant with a further increase of potential. However, no absorption band was observed at 750 nm as reported in [57] for potentiodynamically synthesized POAP films. The behaviour of the *in situ* UV-Vis spectra of POAP films potentiostatically synthesized presented in [9] indicates that the redox transition of POAP from its completely reduced state to its completely oxidized state proceeds through two consecutive reactions in which a charged intermediate species takes part.

4. Spectroscopic Studies of POAP Films Synthesized in Basic and Neutral Media

Jackowska and co-workers [59, 60] studied the chemical and electrochemical oxidation of *o*-AP over a wide pH range employing surface-enhanced raman scattering (SERS) measurements. A mixture of at least eight different compounds was obtained from the chemical oxidation of *o*-AP, and they were separated chromatographically in [59], and then their surface enhanced raman scattering (SERS) spectra were compared. 3-APZ (3-aminophenoxazone) was identified as the main product by recording an IR spectrum, and the second product of the chemical oxidation of *o*-AP was identified as 2-2′-dihydroxyazobenzene (DHAB). 3APZ was considered to be formed by the simultaneous N–C and O–C coupling of *o*-AP monomer units. The N–N coupling yields DHAB. With regard to the solution pH, while DHAB is formed mainly in neutral and basic solutions of *o*-AP, at low pH values, 3APZ was considered to be the main oxidation product.

Jackowska and co-workers [59, 60] also combined SERS measurements with cyclic voltammetry to study the electrochemical formation of POAP at different pH values. Cyclic voltammetric curves for a silver electrode in 0.1 M $LiClO_4$ solutions of *o*-AP at different pHvalues were recorded. In all cases, one pair of redox peaks was observed. However, two pH ranges with different curve features could be distinguished. Within the range of moderate pH (9.1 and 7.2), potentials of anodic (E_{pa}) and cathodic (E_{pc}) peaks changed slightly with pH. However, within the second pH range (pH 3.6 and below), E_{pa} and E_{pc} were strongly pH dependent. These different features of the cyclic voltammetry curves within these two pH ranges were attributed to the presence of two different electroactive oxidation products on the surface of the silver electrode. In order to identify the products formed during the potential cycling, cyclic voltammograms were recorded in different solutions of 0.1 M $LiClO_4$: (i) saturated with nitrosobenzene (pH 10, 6.7, 3.6, and 1.3), (ii) saturated with azoxybenzene (pH 10, 7.0, 3.7, and 2.0), and (iii) on a roughened silver electrode modified with 3-APZ. In the first two cases, no redox peaks were found in the potential range from 0.15 to −0.5 V (SCE) for nitrosobenzene (pH 1.3) and azoxybenzene (pH 2.0) solutions. However, for nitrosobenzene solutions with pH values in the range 10–3.6, two pairs of slightly pH-dependent redox peaks were recorded. The first pair of redox peaks was assigned to the well-known reduction reaction of nitrosobenzene (C_6H_5NO)

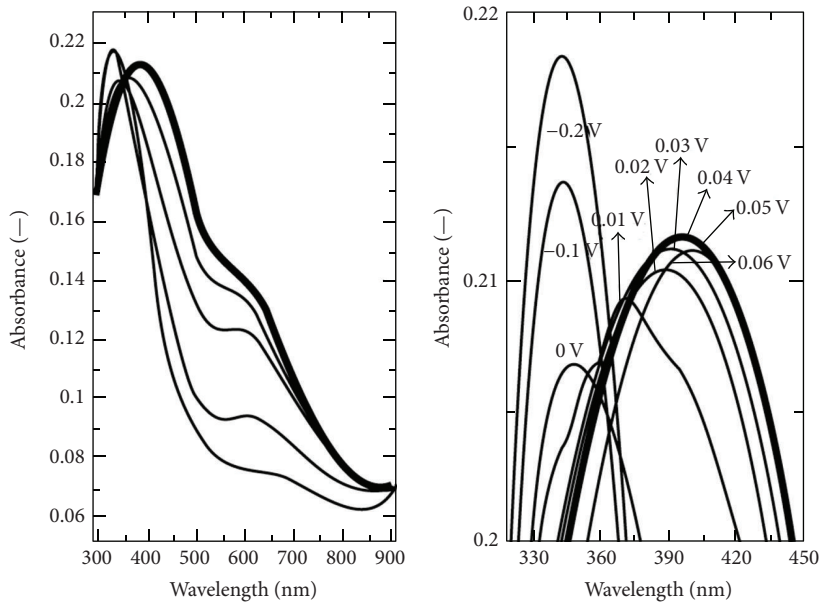

FIGURE 21: (a) *In situ* UV-Vis spectra of POAP at different applied electrode potentials. The POAP film was prepared on ITO-coated glass at 0.8 V (1 h electrolysis) from a solution containing 0.05 M *o*-AP in 0.5 M H_2SO_4 solution. (b) Enlarged spectra of (a) between 320 and 450 nm [9].

to phenylhydroxylamine (C_6H_5NHOH) and the reoxidation of C_6H_5NO to C_6H_5NHOH. The second pair of redox peaks was attributed to the reduction of azoxy species, which are formed by the chemical reaction of C_6H_5NO and C_6H_5NHOH to hydrazobenzene and re-oxidation of hydrazobenzene to azobenzene. In solutions containing azoxybenzene, only one pair of redox peaks was recorded. As it is well known that azoxybenzene can undergo irreversible reduction to azobenzene followed by a two-electron reversible reduction to hydrazobenzene, the observed pair of redox peaks was ascribed to an azo-hydrazo redox reaction. Cyclic voltammetry curves for nitrosobenzene, azoxybenzene, and *o*-AP solutions at moderate pH (about 7) were also compared in [59]. As a pair of redox peaks was obtained for *o*-AP solutions in neutral and alkaline media, it was attributed to the azo-hydrazo couple. Thus, Kudelski and co-workers [59] propose that after oxidation of *o*-AP to *o*-$AP^{\bullet+}$ in neutral and alkaline media, dimerization of *o*-$AP^{\bullet+}$ by N–N coupling takes place. Then, the formation of azo species from *o*-AP on the silver electrode in an alkaline medium was postulated, and the reaction path was considered to be similar to that proposed for the formation of azobenzene from the aniline molecule (Figure 22).

In order to interpret the cyclic voltammetry curves for *o*-AP solutions at pH < 4, cyclic voltammograms for a roughened silver electrode modified with 3-APZ (Ag/3-APZ) were analyzed in the potential range from −0.2 to −0.4 V (SCE). Only one pair of reversible redox peaks was observed on the curves. The dependence of the peak potentials on pH indicated that protons are essential for the electrode reaction. It was not possible to determine E_{pa} and E_{pc} precisely for the Ag/3-APZ electrode at pH < 2, since E_p is in the potential range of silver oxidation, but data obtained for Pt/3-APZ electrode at pH < 3 suggested that E_p changes at a rate of about 60 mV/pH. This relationship indicates that protons and electrons take part in the electrode reaction of 3-APZ in a 1 : 1 ratio. As the voltammetric curves for *o*-AP and Ag/3-APZ electrodes in solutions of pH < 4 were found to be similar, it was postulated in [59] that in more acidic solutions the favoured path after oxidation of *o*-AP to *o*-$AP^{\bullet+}$ is dimerization of *o*-$AP^{\bullet+}$ with N–C coupling resulting in the cyclic dimer 3-APZ.

In order to verify the hypothesis concerning the postulated species on a silver electrode, the SERS spectra of a silver electrode immersed in *o*-AP solution of different pHand electrode potential values were examined in [59]. A band at 1395 cm^{-1} is clearly observed in all spectra. This band was assigned to nitrosophenol and is pH dependent. As can be seen from Figure 23, while this band exhibits a strong intensity in alkaline solutions, it is weaker in the acidic medium. As a similar band at 1390 cm^{-1} is observed in the SERS and resonance Raman spectra of many azo dyes, this band was assigned to the N=N stretching vibration. As was suggested in [59] that the amount of azo species created on the silver electrode surface should be much greater at higher pH values, then, it was concluded that at open-circuit potential, *o*-AP on the silver electrode is already oxidized into two major products: 3-APZ and DHAB. With regard to the potential dependence of the SERS spectrum of an *o*-AP solution, it was observed in [59] that at pH 3.0 (Figure 23(a)) the spectrum is the most intense at the stationary potential electrode E = 0.01 V, weak at −0.2 V, and almost absent at −0.4 V after the reduction of 3-APZ. At pH 7.5 (Figure 23(b)), the overall intensity of the spectrum significantly diminishes

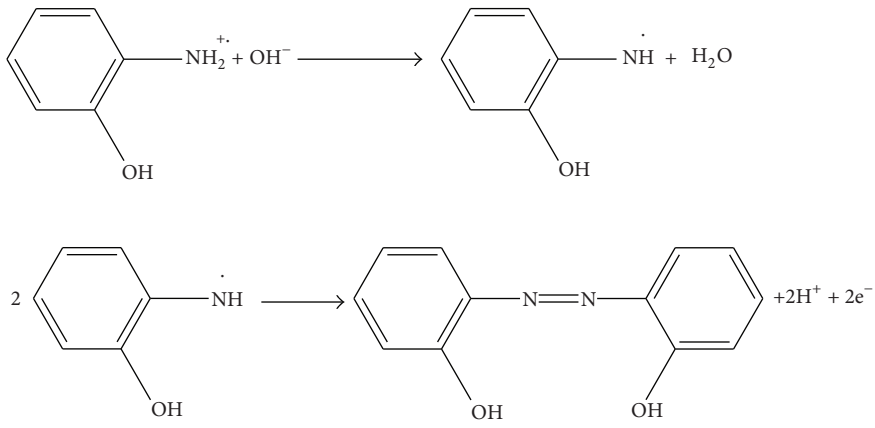

Figure 22: Formation of azo species from *o*-AP on the silver electrode in an alkaline medium [59].

at more negative potential values (about −0.6 V). In alkaline solutions (Figure 23(c)), the main bands ascribed to 3-APZ and DHAB disappear at −0.7 V after a reduction of azo compounds to hydrazo compounds. The spectrum observed at more negative potential values in neutral and alkaline pH was attributed to hydrazo species, which are products of the reduction of DHAB.

The presence of DHAB and 3-APZ in *o*-AP solutions of moderate pH was also reported in [13]. The chemical and electrochemical syntheses of POAP from 0.1 M phosphate buffer solutions (pH 5.5) in the presence and in the absence of the enzyme laccase were studied by Raman and UV spectroscopy in [13]. It was demonstrated that laccase can be utilized as a polymerization initiator with no need of electrochemical monomer oxidation. Raman spectra of POAP electrodeposited at pH 5.5 with and without the presence of laccase, in the polymerization bath and the spectrum of the POAP obtained by the enzyme polymerization of *o*-AP were compared in [13]. Raman bands of 2,2′-dihydroxyazobenzene (DHAB) and 3-aminophenoxazone (3-APZ) were observed in the spectra obtained at pH 5.5. The electrochemically synthesized POAP film shows a strong band at 1397 cm^{-1} that was attributed to the N=N stretching mode of DHBA. This band is weaker in the spectrum of the POAP film electrodeposited in the presence of laccase and it disappears completely in the spectrum of POAP obtained by enzymatic polymerization of *o*-AP. This effect was attributed to the fact that N–N coupling only occurs during the electrochemical oxidation of *o*-AP. Several 3-APZ modes were also observed in the spectra of the three POAP samples (578, 1150, 1278, 1475, 1505, 1605, and 1660 cm^{-1}). Slight shifts in band positions were attributed to further oxidative polymerization of 3-APZ to POAP. Since the POAP structure contains conjugated double bonds, shifts of aromatic ring modes were considered probable. Although the presence of laccase in the electrodeposited POAP films was confirmed by a test using syringaldazine, its contribution to Raman spectra seems to be very weak. Only weak features at 468 and 1264 cm^{-1} were assigned to the enzyme. The spectrum of enzymatically synthesized POAP shows a quite strong band at 1504 cm^{-1}, whose frequency is identical to that of the aromatic ring mode of 3-APZ. As this frequency also coincides with the primary amine deformation mode of *o*-AP, it was suggested that it is related to either monomer that did not react with 3-APZ or short oligomers. Typical UV-visible spectra of POAP electrodeposited in the presence and in the absence of laccase are also shown in [13]. Both spectra are characterized by a broad absorption band with maxima at 445 nm and 430 nm for the film obtained in the presence and in the absence of laccase, respectively. As similar bands were observed for potentiostatically (410 nm) [9] and potentiodynamically (440 nm) [57] electrodeposited POAP films, the bands at 445 nm and 430 nm in [13] were attributed to conjugated π bonds of POAP. The small difference in the position of the bands was related to possible differences in the chain lengths of POAP prepared in the presence and in the absence of laccase.

The electropolymerization of *o*-AP in alkaline media (pH = 12) on copper electrodes employing IR spectrometry was studied in [12]. The IR spectrum of the POAP film and that of the 2-aminophenol compound were compared. The film spectrum did not present the O–H band (3375 cm^{-1} for the stretching vibration and 1268 cm^{-1} for the bonding vibration) characteristic of the 2-aminophenol. Instead of these bands, that of C–O–C at 1297.7 cm^{-1} was observed. This spectral difference was considered to be consistent with an electropolymerization process of *o*-AP, which proceeds through the anodic oxidation of the monomer. The absence of the band at 1700 cm^{-1}, assigned to C=O groups, confirmed the only formation of a polyether compound. The presence of the characteristic strong absorptions corresponding to the bands of the $-NH_2$ group in the ranges 300–3500 cm^{-1} and 1590–1610 cm^{-1} was observed in the IR spectra of the films. The ESCA analysis of POAP films was also carried out in [12]. The spectrum of the oxygen 1s was interpreted as being composed of different peaks at 531.5, 532.9, and

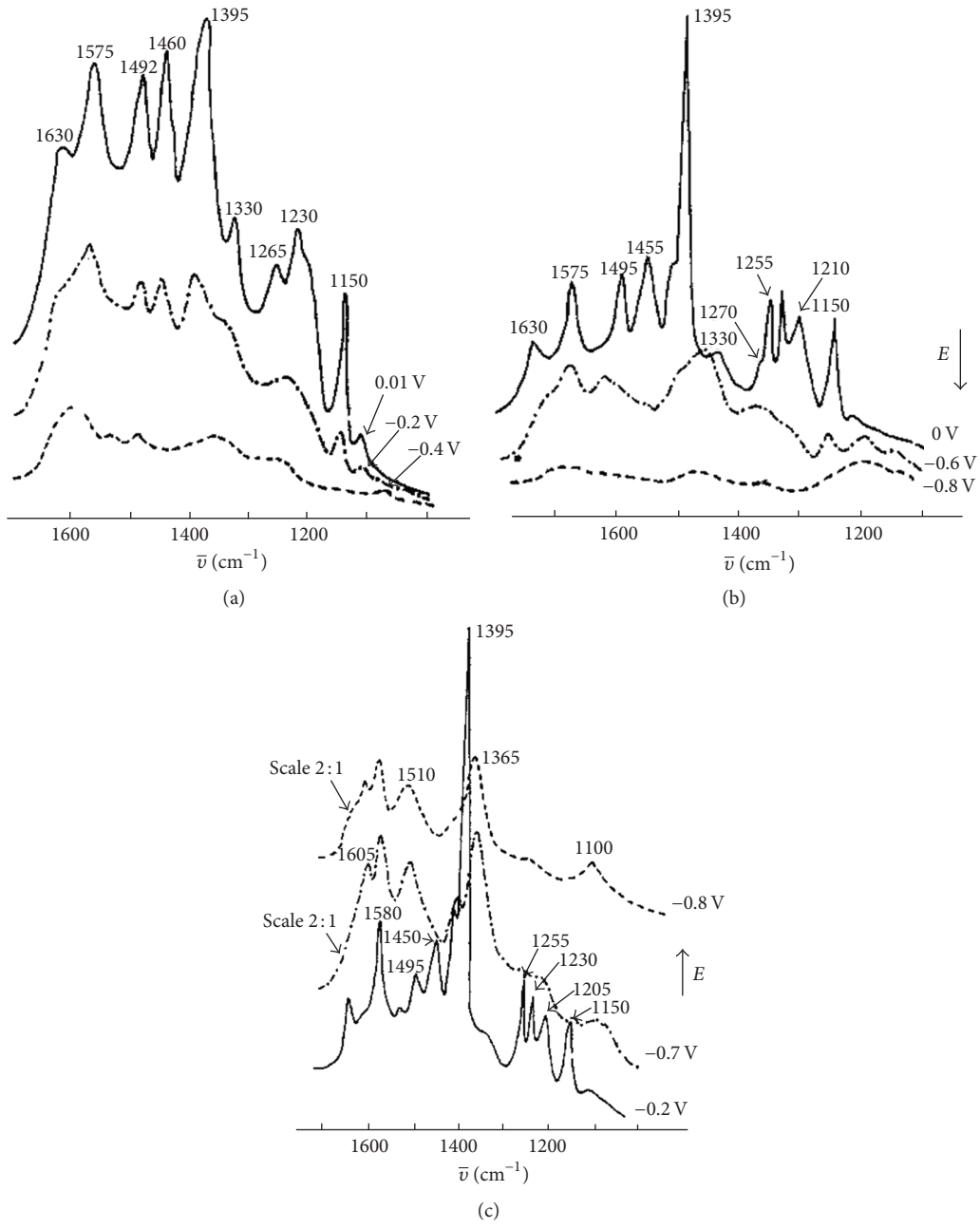

Figure 23: SERS spectra of *o*-AP solutions at (a) pH 3.0, (b) pH 7.5, and (c) pH 9.7, for different electrode potentials [59].

533.9 eV, attributed to oxygen bonding to a metal in an oxide, to oxygen of water adsorbed molecules or hydroxide group (OH), and to C–O–C bonds, respectively. The third component at high energy (286.5 eV) of the C_{1s} spectrum was assigned to C–O–C bonds, while the low energy components were considered to be characteristic of C–C bonds (284.6 eV) and C-N bonds (285.5 eV). The N_{1s} spectrum was assigned to the three types of bonds of the 2-aminophenol: O–N, N–H, and C–N (389.9, 400.3, and 401.2 eV). Copper in its oxidized forms was also observed in the film: Cu_2O (932.6 eV) and CuO (933.7 eV). The higher energy component (934.5 eV) was attributed to a complex formed with the organic compounds. It is concluded in [12] that the POAP film growth process in alkaline media involves the deprotonation of the aminophenol molecule, which is probably chemisorbed at the metal surface, followed by oxidation and electropolymerization reactions. In this whole process, the polymerization affects the –OH group by the formation of the C–O–C bond, while the $-NH_2$ groups are preserved.

5. Summary and Concluding Remarks

Electro-oxidation of *ortho*-aminophenol (*o*-AP) from basic and acidic solutions leads to the formation of poly(*o*-aminophenol) (POAP). With regard to products of *o*-AP oxidation,

SERS measurements [59] indicate that while 2-2′-dihydroxyazobenzene (DHAB) is formed mainly in neutral and basic solutions, at low pH values 3-aminophenoxazone (3APZ) is the main electro-oxidation product. It was postulated that after oxidation of *o*-AP to *o*-$AP^{\bullet+}$ in neutral and alkaline media, dimerization of *o*-$AP^{\bullet+}$ by N–N coupling takes place. The N–N coupling yields DHAB. The favoured path after oxidation of *o*-AP to *o*-$AP^{\bullet+}$ in more acidic solutions (pH < 4) is dimerization of *o*-$AP^{\bullet+}$ with N–C coupling resulting in the cyclic dimer 3-APZ.

On the basis of chemical synthesis and spectroscopic techniques, different structures have been proposed for POAP synthesized in acid medium. Barbero et al. [1] propose that oxidation of 3APZ leads to a ladder structure polymer with phenoxazine units. However, Barbero et al. indicate that the *o*-$AP^{\bullet+}$ radical may also be dimerized by C–C coupling. Thus, the formation of a composite of two different films, one of linear chain structure similar to polyaniline (PANI) and the other with a phenoxazine-like chain structure, was assumed to be possible for POAP in [1]. However, Barbero et al. [1] remark on the absence of the characteristic strong absorption of the carbonyl group and that of the phenol group in the IR spectrum of POAP. The absence of the carbonyl band was considered to be an indication of an insignificant quantity of *o*-quinone in the film. In the same way, the absence of an important hydroxyl group absorption band was attributed to a low proportion of a possible linear chain polymer structure. Then, a film with a phenoxazine-like chain structure was considered as the predominant product obtained by electro-oxidation of *o*-AP in acid solutions. The POAP structure was also studied in [1] by *in situ* UV-visible spectroscopy. As the UV-Vis spectrum has the same characteristics as that reported for 3APZ, it was considered as a confirmation that the film is composed of phenoxazine-like units. The chemical synthesis of POAP confirmed that the actual monomer in the formation of the polymer is the cyclic dimer of *o*-AP, 3APZ. Salavagione et al. [49] studied the POAP structure employing FTIR spectroscopy. As bands corresponding to structures, where the polymer remains linear and the –OH groups are free and could be oxidized to *ortho*-quinonimines, were not observed, in agreement with Barbero et al. [1], it was concluded in [49] that the most probable structure of the polymer formed in the oxidation of *o*-AP contains the phenoxazine unit as the main constituent of its structure. On the basis of IR spectrometry and voltammetry, Gonçalves and co-workers [4] conclude that despite the fact that POAP films may present phenoxazine units and then similar redox responses can be expected for POAP films and 3APZ-modified electrodes, 3APZ does not polymerize. Gonçalves and co-workers [4] postulate that the electrochemical oxidation of *o*-AP consists of a first oxidation step involving a two-electron transfer to form radical cations followed by chemical couplings of radical cation-radical cation or radical-monomer species (E(CE)) mechanism to form a ladder polymer with phenoxazine units. However, radical cations can also react quickly near the electrode surface, and after the first step involving two electrons, soluble products are easily formed by hydrolysis. Thus, besides a film with a ladder structure, Gonçalves and co-workers [4] propose that the oxidation of *o*-AP can produce intermediate benzoquinone monoamine after successive cycling. Particularly at less controlled conditions such as at higher final potentials and low scan rates, monoamines can react with neutral *o*-AP giving an intermediate (2-amino-*o*-indopHenol) prior to cyclization to 3APZ.

Besides a completely ring-closed structure with phenoxazine units, other different structures have been proposed for POAP. Kunimura and co-workers [6] compared the IR spectra of POAP, *o*-AP, and phenoxazine. The peak at 1645 cm^{-1} observed in the POAP spectrum, and also in the phenoxazine spectrum, was assigned to the stretching of the C=N bonds present in a ladder polymer with phenoxazine rings. However, also the peaks due to the N–H stretching vibrations of the imino group of the POAP film and phenoxazine were observed at 3420 cm^{-1}. The presence of a relatively strong absorption peak at around 3420 cm^{-1} was considered as an indication that POAP does not possess a completely ring-closed structure, as proposed in [1]. Then, a partially ring-opened structure as that shown in Figure 11 was also proposed for POAP [6]. Furthermore, from the fact that the absorption peak, which is assigned to the stretching vibration of the C=O bonds of aromatic keto groups, was observed at 1670 cm^{-1}, not only the partially ring-opened structure shown in Figure 11 was proposed for POAP in [6], but also the structure shown in Figure 12, which was assumed to proceed from a polymerization via C–N=C bonds, was proposed as possible structure of POAP. UV and Raman studies carried out by Zhang et al. [7] show that the POAP matrix consists of both oxidized (quinonoid) and reduced (N-pHenyl-*p*-phenylenediamine) monomer repeating units. The structure of POAP shown in Figure 13 allows explaining the interaction of POAP with metal cations. The cation capture process was attributed to the simultaneous presence of hydroxyl and amino groups of the polymeric backbone of POAP, in which the lone pair electrons are available to coordinate with metal cations.

With regard to electrosynthesis conditions, different redox pairs are observed in the cyclic voltammograms during potentiodynamic POAP deposition. While the less positive redox pair was associated with the redox reactions of *o*-AP polymers, most positive redox pairs were attributed to the oxidation of *o*-AP to the radical cation ($OAP^{\bullet+}$) and its further oxidation to the dication, respectively. It is indicated that POAP growth proceeds mainly through the reactions between the growing polymer and oxidized monomer units, and subsequent cyclization of the functional units in the polymer leads to a ladder structure. The flattening of more positive peak systems during the polymer synthesis was attributed to a limitation to *o*-AP diffusion during the polymerization process. The scarce formation of the radical cation (polaron) and dication (bipolaron) during the polymerization was associated with restricted charge-transport processes and electron delocalization effects along a partly cross-linked polymer chain. In this regard, some differences between POAP and PANI electrodeposition can be remarked. While the deposition of POAP proceeds mainly through the direct oxidation of the monomer, in the polymerization of aniline, the oxidized

monomers (nitrenium cations), which are reactive towards the phenazine rings in aromatic electrophilic substitutions, are only produced at high potential values and low aniline concentration. As a result, PANI polymers of a different structure as compared with POAP should be formed. Also, the easy formation of radical cations from the oxidation of *o*-AP differentiates the electropolymerization of *o*-AP from that of aniline and its other derivatives such as metanieic acid. The presence of the electron-donating OH group in *o*-AP facilitates monomer oxidation, whereas metanilic acid is difficult to oxidize because of the presence of an electron-withdrawing SO_3 group. In this case, aniline must be added to produce sufficient dications to sustain polymer growth. With regard to caption capture, the Ag^+-POAP complex was also compared with Ag^+-PANI. The Ag^+-POAP complex presents an improved stability over that of Ag^+-PANI due to the cooperative action of the oxygen atom in the POAP chemical structure. Besides, the redox reaction of silver is within the range of the POAP redox reaction, and, then, changes of POAP conductivity were not significant during the redox reactions of the POAP-Ag^+ complex. This was very different from the situation of the Ag^+-PANI complex, where the redox switching of PANI between the insulating state of leucoemeraldine and the conducting state of emeraldine has substantial influence on the voltammetric response of silver redox behaviour. Also, it has been demonstrated that POAP can capture silver four times more than PANI and is more resistant than PANI to electrochemical degradation.

Structural changes during the redox process of potentiodynamically synthesized POAP films were studied by coupling cyclic voltammetry with UV-Vis [57], Raman [58], and FTIR spectroscopy [9]. ERS measurements were also employed to characterize the redox process of POAP [2]. Different electrochemical and spectroscopic studies indicate that the mechanism of the redox process of POAP involves a charged intermediate when the polymeric film is changed from the reduced state to the oxidized one. The redox reaction of POAP was considered by some researchers [7] as an internal conversion represented by the stoichiometry given in Figure 14. That is, the polarization of POAP at potential values more positive than 0.1 V (SCE) transforms the polymer predominately into the quinonoid form, whereas the reduced (*N*-phenyl-*p*-phenylenediamine) units predominate at more negative potentials. An increase of potential increases the extent of oxidation, but Raman spectroscopy indicates that the oxidation is not complete even at 0.5–0.6 V (SCE). A broad absorption band extending from 410 nm to 532 nm was also observed when the POAP film was polarized in the potential range 0.1–1.1 V (SCE) [7]. This band was attributed to the formation of radical cations as the polymer is oxidized, and it was associated with π-π^* transitions from both oxidized (quinonoid) units and the reduced (*N*-phenyl-*p*-phenylenediamine) units. The absence of differentiable absorption peaks within the wavelength 410 nm to 532 nm implies that π-π^* transitions occur at very close frequencies. In other papers, the redox process of POAP was interpreted in terms of the oxidation of amine groups to imine groups [57]. In this regard, absorbance changes in the wavelength region comprised between 300 nm and 800 nm were employed in [57] to study the redox switching of POAP. Three bands were studied: 340 nm, 450 nm and 750 nm. The band at 340 nm was attributed to the phenoxazine structure of the polymer. The band at 450 nm was assigned to the partially oxidized phenoxazine structure. With regard to the band in the region of λ ~750 nm, the absorbance first increases with potential up to $E = 0.1$ V, and then, for $E > 0.1$ V, the absorbance decreases. At $\lambda = 750$ nm the absorbance presents a maximum at $E = 0.15$ V, and it was considered to be indicative of the existence of a transient species. Raman spectroscopy and voltammetry were also combined to study the existence of intermediate species during the redox process of POAP. The observed band at 1638 cm^{-1} [58] was attributed to –C=N– in quinonimine units. The behaviour of the band with the applied potential shows that when the potential increases, the band at 1638 cm^{-1} also increases until a potential of about 0.2 V, and thereafter, it diminishes. The behaviour of the band at 1638 cm^{-1} was also attributed to a typical intermediate species. The existence of intermediate species was explained on the basis of an oxidation process that occurs through two consecutive reactions from the totally reduced phenoxazine form to the completely oxidized one, through a charged species, which was considered to be a cation radical. Intermediate species in the conducting potential range of POAP were also observed by electron spin resonance measurements [2]. The maximum in ESR spectra for POAP occurs in the potential ranging from −0.24 to approximately 0.0 V (SCE). The decrease and further absence of a detectable ESR signal at potentials higher than 0.55 V were attributed to a combination of radicals to give rise to dication species, which are not ESR active because of their paired spin.

Cyclic voltammograms of POAP films potentiostatically synthesized at relatively low potentials (E = 0.7–0.8 V (SCE)) exhibit two redox processes with midpoint potential between the respective redox potentials ($E = 0.29$ V/SCE) showing that the transition of POAP between the reduced form and the oxidized form occurs via two consecutive reactions [9]. Although the Raman features of the POAP films potentiostatically and potentiodynamically synthesized were similar, marked differences with respect to the potential dependence of some bands were observed [9]. A difference was observed particularly with respect to the potential dependence of the band at around 1645 cm^{-1}. The band was assigned to –C=N– in quinonimine units and was considered in [9] to correspond to the C–N–C bond of a heterocyclic six-membered ring structure arising from *ortho*-coupling rather than *para*-coupling during the electropolymerization, resulting in a ladder polymer. The intensity of this band sharply increased at 0.3 V and slowly decreased at more positive potentials for the POAP film potentiostatically synthesized. However, in the case of potentiodynamically prepared POAP, this band attained the intensity maximum at about $E = 0.2$ V. As this band did not disappear even at the highest applied potential, the oxidation of fully reduced POAP synthesised potentiostatically to fully oxidized POAP was assumed to proceed via an intermediate half-oxidized state. Despite the fact that voltammetric measurements in acid solutions of low

concentration indicate that the redox process of potentiodynamically synthesized POAP films involves only one redox couple, recent studies in $HClO_4$ solutions of high concentration (5 M) [58] show the existence of two redox processes during the redox conversion of POAP. In this regard, spectroscopic and optic *in situ* techniques coupled with voltammetric measurements suggest that the redox mechanism of potentiodynamically synthesized POAP films involves two steps. The first step, at less positive potentials, mainly involves the anion exchange, whereas in the second step, at more positive potentials, the insertion/expulsion of protons is produced.

With regard to a critical view of the different results reported in this review about the electropolymerization reaction of *o*-AP and the structures proposed for electrosynthesized POAP films, in the opinion of the authors it is very important to know which molecular structure is appropriate to interpret the results obtained in each work. In this regard, in previous papers [61, 62], one of the authors of this work studied the POAP deactivation caused by the ferric cation capture by employing rotating disc electrode voltammetry [61] and impedance spectroscopy [62]. The cation capture process by a POAP film is more frequently explained on the basis of the 1,4-substituted structure given in Figure 13 because of the simultaneous presence of hydroxyl and amino groups on the polymeric backbone. However, it is interesting to remark that although the synthesis method employed in [61, 62] was the same as that employed in other spectroelectrochemical studies of POAP [57], the optical results obtained in [57] were adequately interpreted in terms of the ladder structure based on phenoxazine units. Then, it is possible that the formation of a composite of polymers with different structures could be taking place during the *o*-AP polymerization. In this regard, extreme care should be taken in the preparation of a POAP film, not only in the concentration, but also in the potential ranges. On the contrary, the possibility of side reactions and consequently "side" polymers increases, and the real structures of the films obtained could be quite complex. However, in our opinion, the critical points are the stability of solutions employed to prepare POAP and the proper stability of the polymer once synthesized. The monomer must be purified. In our works, *o*-AP was purified by recrystallizing it twice in ethyl acetate. The pale yellow plates were then stored in a desiccator under vacuum. Within two days before use, a further recrystallization in benzene was performed and the colourless needles were stored in a nitrogen atmosphere until use. The needles had a melting point of 172°C. Also, it should also be kept in mind that POAP degrades quite easily. The effect of degradation on the charge-transport process of POAP films was reported by some of the authors of the present work in different papers [16–18, 21, 22, 63]. In this regard, the impedance diagram of a recently prepared POAP film exhibits a Warburg region; however, after prolonged potential cycling or storage, the impedance diagram starts to show a high-frequency semicircle, which is indicative of the development of an interfacial resistance at the metal-polymer interface which, in turn, decreases the film conductivity. This effect is also accompanied by a gradual attenuation of the voltammetric response of the polymer film. However, it is more visible from the impedance response of the film. The conductivity decrease of POAP was interpreted in terms of an electron "hopping" mechanism, where deactivation of redox sites of the polymer causes an increase in the electron "hopping" distance between redox centers [63]. The main degradation product of POAP should be a benzoquinone derivative as in the case of PANI. Then, certainly, some amount of free C-OH and C=O groups might be present in the reduced and oxidized polymer, respectively, according to experimental conditions under which the results are obtained (prolonged potential cycling, positive potential limit, storage time without use, etc.). Then, according to these authors, there are matters relative to POAP stability that remain to be clarified and strongly affect the properties and structure of electrochemically synthesized POAP films.

Acknowledgments

The authors gratefully acknowledge the Consejo Nacional de Investigaciones Científicas y Técnicas (CONICET) and also the Facultad de Ciencias Exactas, Universidad Nacional de La Plata (UNLP).

References

[1] C. Barbero, J. J. Silber, and L. Sereno, "Formation of a novel electroactive film by electropolymerization of ortho-aminophenol. Study of its chemical structure and formation mechanism. Electropolymerization of analogous compounds," *Journal of Electroanalytical Chemistry*, vol. 263, no. 2, pp. 333–352, 1989.

[2] J. M. Ortega, "Conducting potential range for poly(o-aminophenol)," *Thin Solid Films*, vol. 371, no. 1, pp. 28–35, 2000.

[3] R. Ojani, J. B. Raoof, and S. Fathi, "Poly(o-aminophenol) film prepared in the presence of sodium dodecyl sulfate: application for nickel ion dispersion and the electrocatalytic oxidation of methanol and ethylene glycol," *Electrochimica Acta*, vol. 54, no. 8, pp. 2190–2196, 2009.

[4] D. Gonçalves, R. C. Faria, M. Yonashiro, and L. O. S. Bulhões, "Electrochemical oxidation of o-aminophenol in aqueous acidic medium: formation of film and soluble products," *Journal of Electroanalytical Chemistry*, vol. 487, no. 2, pp. 90–99, 2000.

[5] Y. Yang and Z. Lin, "Effects of surface oxide species on the electropolymerization of o-aminophenol on pretreated glassy carbon electrodes," *Synthetic Metals*, vol. 78, no. 2, pp. 111–115, 1996.

[6] S. Kunimura, T. Ohsaka, and N. Oyama, "Preparation of thin polymeric films on electrode surfaces by electropolymerization of o-aminophenol," *Macromolecules*, vol. 21, no. 4, pp. 894–900, 1988.

[7] A. Q. Zhang, C. Q. Cui, Y. Z. Chen, and J. Y. Lee, "Synthesis and electrochromic properties of poly-o-aminophenol," *Journal of Electroanalytical Chemistry*, vol. 373, no. 1-2, pp. 115–121, 1994.

[8] A. Q. Zhang, C. Q. Cui, and J. Y. Lee, "Metal-polymer interactions in the Ag^+/poly-*o*-aminophenol system," *Journal of Electroanalytical Chemistry*, vol. 413, no. 1-2, pp. 143–151, 1996.

[9] A. U. H. A. Shah and R. Holze, "Poly(o-aminophenol) with two redox processes: a spectroelectrochemical study," *Journal of Electroanalytical Chemistry*, vol. 597, no. 2, pp. 95–102, 2006.

[10] M. C. Miras, A. Badano, M. M. Bruno, and C. Barbero, "Nitric oxide electrochemical sensors based on hybrid films of conducting polymers and metal phtalocyanines," *Portugaliae Electrochimica Acta*, vol. 21, pp. 235–243, 2003.

[11] S. M. Golabi and A. Nozad, "Electrocatalytic oxidation of methanol at lower potentials on glassy carbon electrode modified by platinum and platinum alloys incorporated in poly(*o*-aminophenol) film," *Electroanalysis*, vol. 15, no. 4, pp. 278–286, 2003.

[12] A. Guenbour, A. Kacemi, A. Benbachir, and L. Aries, "Electropolymerization of 2-aminophenol. Electrochemical and spectroscopic studies," *Progress in Organic Coatings*, vol. 38, no. 2, pp. 121–126, 2000.

[13] B. Pałys, M. Marzec, and J. Rogalski, "Poly-o-aminophenol as a laccase mediator and influence of the enzyme on the polymer electrodeposition," *Bioelectrochemistry*, vol. 80, no. 1, pp. 43–48, 2010.

[14] C. Barbero, J. J. Silber, and L. Sereno, "Electrochemical properties of poly-ortho-aminophenol modified electrodes in aqueous acid solutions," *Journal of Electroanalytical Chemistry*, vol. 291, no. 1-2, pp. 81–101, 1990.

[15] T. Komura, Y. Ito, T. Yamaguti, and K. Takahasi, "Charge-transport processes at poly-o-aminophenol film electrodes: electron hopping accompanied by proton exchange," *Electrochimica Acta*, vol. 43, no. 7, pp. 723–731, 1997.

[16] R. Tucceri, "A review about the charge conduction process at poly(*o*-aminophenol) film electrodes," *The Open Physical Chemistry Journal*, vol. 4, pp. 62–77, 2010.

[17] F. J. Rodríguez Nieto and R. I. Tucceri, "The effect of pH on the charge transport at redox polymer-modified electrodes: an AC impedance study applied to poly(o-aminophenol) film electrodes," *Journal of Electroanalytical Chemistry*, vol. 416, no. 1-2, pp. 1–24, 1996.

[18] C. Barbero, R. I. Tucceri, D. Posadas, J. J. Silber, and L. Sereno, "Impedance characteristics of poly-o-aminophenol electrodes," *Electrochimica Acta*, vol. 40, no. 8, pp. 1037–1040, 1995.

[19] R. I. Tucceri, "Surface resistance measurements on thin gold film electrodes coated with poly(o-aminophenol) films," *Journal of Electroanalytical Chemistry*, vol. 505, no. 1-2, pp. 72–84, 2001.

[20] O. Levin, V. Kondratiev, and V. Malev, "Charge transfer processes at poly-o-phenylenediamine and poly-o-aminophenol films," *Electrochimica Acta*, vol. 50, no. 7-8, pp. 1573–1585, 2005.

[21] J. F. Rodriguez Nieto, R. I. Tucceri, and D. Posadas, "EIS detection of the partial oxidation of polymers derived from aryl amines," *Journal of Electroanalytical Chemistry*, vol. 403, no. 1-2, pp. 241–244, 1996.

[22] R. Tucceri, "The effect of high positive potentials on the different charge transport and charge transfer parameters of poly(o-amnophenol) modified electrodes. A study using cyclic voltammetry, steady-state rotating disc electrode voltammetry and AC impedance measurements," *Journal of New Materials for Electrochemical Systems*, vol. 8, no. 4, pp. 305–315, 2005.

[23] R. Tucceri, "A review about the surface resistance technique in electrochemistry," *Surface Science Reports*, vol. 56, no. 3-4, pp. 85–157, 2004.

[24] A. G. MacDiarmid and R. B. Kaner, in *Handbook of Conducting Polymers*, T. A. Skotheim, Ed., vol. 1, p. 689, Marcel Dekker, New York, NY, USA, 1986.

[25] R. B. Kaner, A. G. MacDiarmid, and R. J. Mammone, "Polyacetylene, (CH)x: an electrode-active material in aqueous and nonaqueous electrolytes," *ACS Symposium Series*, vol. 242, pp. 575–584, 1984.

[26] E. Dalas, "Novel dry cells constructed solely from polymers," *Solid State Communications*, vol. 77, no. 1, pp. 63–64, 1991.

[27] W. S. Huang, B. D. Humphrey, and A. G. MacDiarmid, "Polyaniline, a novel conducting polymer. Morphology and chemistry of its oxidation and reduction in aqueous electrolytes," *Journal of the Chemical Society, Faraday Transactions 1*, vol. 82, no. 8, pp. 2385–2400, 1986.

[28] T. Nakajima and T. Kawagoe, "Polyaniline: structural analysis and application for battery," *Synthetic Metals*, vol. 28, no. 1-2, pp. 629–638, 1989.

[29] F. Beck, T. Boinowitz, and U. Tormin, "Rechargeable batteries in aqueous electrolytes," *DECHEMA Monographs*, vol. 128, p. 287, 1983.

[30] K. Nishio, M. Fujimoto, N. Yoshinaga et al., "Characteristics of a lithium secondary battery using chemically-synthesized conductive polymers," *Journal of Power Sources*, vol. 34, no. 2, pp. 153–160, 1991.

[31] A. P. Chattaraj and I. N. Basumallick, "Improved conducting polymer cathodes for lithium batteries," *Journal of Power Sources*, vol. 45, no. 2, pp. 237–242, 1993.

[32] K. Tanaka, T. Shichiri, and T. Yamabe, "Influence of polymerization temperature on the characteristics of polythiophene films," *Synthetic Metals*, vol. 16, no. 2, pp. 207–214, 1986.

[33] M. Satoh, K. Kaneto, and K. Yoshino, "Electrochemical preparation of high quality poly(*p*-phenylene) film," *Journal of the Chemical Society, Chemical Communications*, no. 22, pp. 1629–1630, 1985.

[34] A. Guerrieri, R. Ciriello, and D. Centonze, "Permselective and enzyme-entrapping behaviours of an electropolymerized, non-conducting, poly(o-aminophenol) thin film-modified electrode: a critical study," *Biosensors and Bioelectronics*, vol. 24, no. 6, pp. 1550–1556, 2009.

[35] C. G. J. Koopal and R. J. M. Nolte, "An amperometric biosensor based on polypyrrole," *Bioelectrochemistry and Bioenergetics*, vol. 33, no. 1, pp. 45–53, 1994.

[36] S. Cosnier and H. Gunther, "A polypyrrole $[RhIIIC_5Me_5(bpy)Cl]^+$ modified electrode for the reduction of NAD^+ cofactor. Application to the enzymatic reduction of pyruvate," *Journal of Electroanalytical Chemistry*, vol. 315, no. 1-2, pp. 307–315, 1991.

[37] N. C. Foulds and C. R. Lowe, "Immobilization of glucose oxidase in ferrocene-modified pyrrole polymers," *Analytical Chemistry*, vol. 60, no. 22, pp. 2473–2478, 1988.

[38] S. Y. Lu, C. F. Li, D. D. Zhang et al., "Electron transfer on an electrode of glucose oxidase immobilized in polyaniline," *Journal of Electroanalytical Chemistry*, vol. 364, no. 1-2, pp. 31–36, 1994.

[39] D. Pan, J. Chen, L. Nie, W. Tao, and S. Yao, "Amperometric glucose biosensor based on immobilization of glucose oxidase in electropolymerized *o*-aminophenol film at Prussian blue-modified platinum electrode," *Electrochimica Acta*, vol. 49, no. 5, pp. 795–801, 2004.

[40] X. Chen, J. Chen, C. Deng et al., "Amperometric glucose biosensor based on boron-doped carbon nanotubes modified electrode," *Talanta*, vol. 76, no. 4, pp. 763–767, 2008.

[41] D. Pan, J. Chen, S. Yao, W. Tao, and L. Nie, "An amperometric glucose biosensor based on glucose oxidase immobilized

in electropolymerized poly(o-aminophenol) and carbon nanotubes composite film on a gold electrode," *Analytical Sciences*, vol. 21, no. 4, pp. 367–371, 2005.

[42] J. Li and X. Lin, "Glucose biosensor based on immobilization of glucose oxidase in poly(*o*-aminophenol) film on polypyrrole-Pt nanocomposite modified glassy carbon electrode," *Biosensors and Bioelectronics*, vol. 22, no. 12, pp. 2898–2905, 2007.

[43] W. Tao, D. Pan, Y. Liu, L. Nie, and S. Yao, "An amperometric hydrogen peroxide sensor based on immobilization of hemoglobin in poly(*o*-aminophenol) film at iron-cobalt hexacyanoferrate-modified gold electrode," *Analytical Biochemistry*, vol. 338, no. 2, pp. 332–340, 2005.

[44] M. A. Valdés García, P. Tuñón Blanco, and A. Ivaska, "A poly(*o*-aminophenol) modified electrode as an amperometric hydrogen peroxide biosensor," *Electrochimica Acta*, vol. 43, no. 23, pp. 3533–3539, 1998.

[45] E. Miland, A. J. Miranda Ordieres, P. Tuñón Blanco, M. R. Smyth, and C. O. Fágáin, "Poly(*o*-aminophenol)-modified bienzyme carbon paste electrode for the detection of uric acid," *Talanta*, vol. 43, no. 5, pp. 785–796, 1996.

[46] M. J. Lobo-Castañón, A. J. Miranda-Ordieres, and P. Tuñón-Blanco, "A bienzyme-poly-(*o*-phenylenediamine)-modified carbon paste electrode for the amperometric detection of L-lactate," *Analytica Chimica Acta*, vol. 346, no. 2, pp. 165–174, 1997.

[47] M. J. Lobo, A. J. Miranda, J. M. López-Fonseca, and P. Tuñón, "Electrocatalytic detection of nicotinamide coenzymes by poly(*o*-aminophenol)—and poly(*o*-phenylenediamine)-modified carbon paste electrodes," *Analytica Chimica Acta*, vol. 325, no. 1-2, pp. 33–42, 1996.

[48] D. Scolari and R. Tucceri, "Some applications of non-conducting poly(*o*-aminophenol) films in Bioelectrochemistry and Electrocatalysis," *Micro and Nanosystems*, vol. 3, pp. 115–130, 2011.

[49] H. J. Salavagione, J. Arias, P. Garcés, E. Morallón, C. Barbero, and J. L. Vázquez, "Spectroelectrochemical study of the oxidation of aminophenols on platinum electrode in acid medium," *Journal of Electroanalytical Chemistry*, vol. 565, no. 2, pp. 375–383, 2004.

[50] Y. Z. Chen, A. Q. Zhang, and Z. W. Tian, "Poly(o-aminophenol) studied by X-ray photoelectron spectroscopy," *Chemical Journal of Chinese Universities*, vol. 12, p. 519, 1991.

[51] L. C. Lee and Y. Q. Zhou, "Structural characterization of emeraldine-salt polyaniline," *Spectroscopy and Spectral Analysis*, vol. 11, p. 12, 1991.

[52] C. Barbero, J. Zerbino, L. Sereno, and D. Posadas, "Optical properties of electropolymerized orthoaminophenol," *Electrochimica Acta*, vol. 32, no. 4, pp. 693–697, 1987.

[53] M. A. Habib and S. P. Maheswari, "Electrochromism of polyaniline: an in situ FTIR study," *Journal of the Electrochemical Society*, vol. 136, no. 4, pp. 1050–1053, 1989.

[54] A. Q. Zhang, Y. Z. Chen, and Z. W. Tian, "Metal-polymer interaction in the Ag^{+}/polyaniline system," *Acta Physica et Chemica*, vol. 9, p. 523, 1993.

[55] J. Yano, H. Kawakami, S. Yamasaki, and Y. Kanno, "Cation capturing ability and the potential response of a poly(*o*-aminophenol) film electrode to dissolved ferric ions," *Journal of the Electrochemical Society*, vol. 148, no. 2, pp. E61–E65, 2001.

[56] J. Yano, H. Kawakami, and S. Yamasaki, "Potential response of poly(o-aminophenol) film electrode to dissolved ferric ion," *Synthetic Metals*, vol. 102, no. 1–3, p. 1335, 1999.

[57] R. I. Tucceri, C. Barbero, J. J. Silber, L. Sereno, and D. Posadas, "Spectroelectrochemical study of poly-o-aminophenol," *Electrochimica Acta*, vol. 42, no. 6, pp. 919–927, 1997.

[58] H. J. Salavagione, J. Arias-Pardilla, J. M. Pérez et al., "Study of redox mechanism of poly(o-aminophenol) using in situ techniques: evidence of two redox processes," *Journal of Electroanalytical Chemistry*, vol. 576, no. 1, pp. 139–145, 2005.

[59] K. Jackowska, J. Bukowska, and A. Kudelski, "Electro-oxidation of o-aminophenol studied by cyclic voltammetry and surface enhanced Raman scattering (SERS)," *Journal of Electroanalytical Chemistry*, vol. 350, no. 1-2, pp. 177–187, 1993.

[60] K. Jackowska, J. Bukowska, and A. Kudelski, "Poly-ortho-aminophenol modified electrodes—structure and electrochemical properties," *Polish Journal of Chemistry*, vol. 68, pp. 141–151, 1994.

[61] R. Tucceri, "Redox mediation and permeation processes at deactivated poly(o-aminophenol) films. A study applying rotating disc electrode voltammetry and electrochemical impedance spectroscopy," *Journal of Electroanalytical Chemistry*, vol. 633, no. 1, pp. 198–206, 2009.

[62] R. Tucceri, "Charge-transfer and charge-transport parameters of deactivated poly(o-aminophenol) film electrodes. A study employing electrochemical impedance spectroscopy," *Journal of Electroanalytical Chemistry*, vol. 659, no. 1, pp. 83–91, 2011.

[63] R. Tucceri, "The change of the electron scattering at the gold film-poly-(*o*-aminophenol) film interface after partial degradation of the polymer film: its relation with the electron transport process within the polymer film," *Journal of Electroanalytical Chemistry*, vol. 562, no. 2, pp. 173–186, 2004.